Master Thesis

Entanglement of the XY spin chain in a random magnetic field

Masashi Fujinaga

January 5, 2007

Department of Physics, Graduate School of Science,
The University of Tokyo,
4-6-1 Komaba, Meguro, Tokyo 153-8505, Japan

Abstract

We study the entanglement of the XY spin chain in a random magnetic field. We are interested in the effect of randomness on the entanglement. We use the concurrence to quantify the entanglement between two spins. We find that: (i) In general, the entanglement is decreased by randomness; (ii) In some regions, the entanglement is restored by a random magnetic field. In particular, we find that the next-nearest-neighbor concurrence in the region $h < J/2$ is restored by a random magnetic field as well as in the region $h > J$, whereas that in the uniform magnetic field at finite temperatures vanishes in the region $h < J/2$; (iii) The qualitative behavior of the concurrence depends on whether the variance of the distribution function is finite or not; the maximum point of the concurrence shifts to the right when the variance of the distribution function is finite, whereas it shifts to the left when the variance of the distribution function is infinite.

Contents

1 Introduction **1**
- 1.1 Entanglement . . . 1
- 1.2 The density matrix . . . 2
  - 1.2.1 The density matrix . . . 3
  - 1.2.2 The reduced density matrix . . . 5
  - 1.2.3 The one-qubit and two-qubit density matrices . . . 6
- 1.3 Definition of an entangled state . . . 7
  - 1.3.1 Definition of a pure entangled state . . . 7
  - 1.3.2 Definition of a mixed entangled state . . . 8
- 1.4 Quantum teleportation . . . 8

2 The von Neumann entropy and the entanglement of formation **11**
- 2.1 The von Neumann entropy . . . 11
- 2.2 The entanglement of formation . . . 12

3 The entanglement of the XY spin chain in a random magnetic field **17**
- 3.1 XY model in a random magnetic field . . . 17
- 3.2 The density matrix of the XY model in a random magnetic field . . . 19
  - 3.2.1 The density matrix . . . 19
  - 3.2.2 Exact solution of the XY model in uniform field . . . 21
  - 3.2.3 Numerical solution of the XY model in a random magnetic field . . . 24
- 3.3 The concurrence . . . 26
  - 3.3.1 Formula for the isotropic XY model . . . 26
  - 3.3.2 The concurrence of the XY model in a uniform field at T . . . 28
  - 3.3.3 The entanglement of the XY model in a random magnetic field . . . 30
  - 3.3.4 The entanglement of the XY model at finite temperature . . . 43

4 Conclusion **47**

A The Schmidt decomposition **49**

B Exact solution of the XY model in a uniform field **51**
- B.1 Diagonalizing Hamiltonian . . . 51

B.2 One-point and two-point correlation functions 55

C Numerical solution of the XY model in a random magnetic field at temperature $T = 0$ **60**
C.1 Diagonalizing the Hamiltonian 60
C.2 One-point and two-point correlation functions at $T = 0$ 62

Bibliography **64**

Chapter 1

Introduction

1.1 Entanglement

In the present thesis, we study the entanglement of the XY spin chain in a random magnetic field. We are interested in the effects of the randomness on the entanglement. The entanglement is a crucial resource for the quantum information processing such as quantum teleportation [1, 2] and superdense coding [3]. In reality, however, the entanglement can be easily destroyed by some decoherence. It is important to know how the entanglement is affected by impurities.

The entanglement is a non-local quantity. This non-locality is a feature of quantum mechanics. Suppose that Alice and Bob share a singlet $|0_A 1_B\rangle - |1_A 0_B\rangle$, where the subscript A indicates that the first particle belongs to Alice and the subscript B indicates that the second particle belongs to Bob. The singlet cannot be expressed as a direct product of the particle A's state and the particle B's state. The situation is said that the particles A and B are entangled. If Alice carries out a measurement, Bob's particle becomes either the state $|0_B\rangle$ or $|1_B\rangle$ immediately. The property that Alice's measurement affects Bob's particle is called non-locality. The non-locality appears because the two particles are entangled.

When the quantum mechanics was born, Einstein, Podolsky, Rosen [4] and Bhom pointed out its non-locality and thought that the quantum mechanics was an incomplete theory because the system A's measurement affects the system B which can be far away from the system A. Moreover, this effect travels faster than the light. Violation of the Bell inequality (CHSH inequality) [5, 6] proved that there exists the non-locality in the actual world. Now, the quantum mechanics is widely accepted, having explained a lot of phenomena which were not explained by classical mechanics. In recent years, the quantum information processing such as quantum teleportation [1, 2], superdense coding [3] and quantum computation [2] were discovered. The entanglement plays a key role in these studies.

In the field of condensed matter physics, many authors have studied the relation between the entanglement and the quantum phase transition [7–11]. Osterloh *et al.* [7] showed that in the transverse Ising model, the entanglement obeys scaling behavior in the vicin-

ity of the phase transition point. Similar work has been done by Osborne and Nielsen [8]. Yano and Nishimori [9,10] showed that the entanglement tells us the phase transition point on the anisotropic anti-ferro-magnetic XY model. Similar work has been done by many authors *e.g* on the extended Hubbard model [11].

Our interest here is the behavior of the entanglement in a noisy environment rather than the relation between the quantum phase transition and the entanglement. The effects of the temperature on the entanglement has been studied [8–10,12]. The entanglement can *increase* as the temperature is increased. We investigate the entanglement of the XY spin-1/2 chain in a random magnetic field and XY spin-1/2 chain in the uniform field at finite temperature. We focus our interest on the entanglement between two spins.

To summarize the present thesis, we find the following:

i) In general, the entanglement decreases as the randomness is increased.

ii) The entanglement in a region of the uniform magnetic field h is enhanced by the random magnetic field, whereas it is not enhanced in the same region by thermal fluctuation.

iii) Qualitative behavior of the entanglement depends on the randomness, in particular, whether the variance of the distribution function is finite or not; see Fig. 1.1. In the case where the variance of the distribution function is finite, the maximum point of the entanglement shifts in the direction of greater uniform magnetic field h as the variance of the distribution function is increased. In the case where the variance is infinite, in contrast, the maximum point first shifts in the direction of less uniform magnetic field.

The present thesis is organized as follows: In Chapter 1, we explain the entangled state, both pure and mixed. Quantum teleportation, which is an application of the entangled state, is also mentioned. In Chapter 2, we review the entanglement measures known as the von Neumann entropy and the concurrence. In the present thesis, we use the concurrence as a measure of the entanglement. In Chapter 3, we numerically study the entanglement of the XYspin chain in a random magnetic field as well as the XYspin chain in the uniform field at finite temperatures.

1.2 The density matrix

In this section, we first define the density matrix. The density matrix can describe a general state of any quantum systems. Next, we consider how to construct one-qubit and two-qubit density matrices, which are necessary to use entanglement measures such as the von Neumann entropy and the entanglement of formation in Chapter 2.

1.2.1 The density matrix

Here, we explain how to describe a quantum state whose state is not completely known, by using the density matrix. Suppose that the state in question is given by an ensemble of the set $\{p_i, |\psi_i\rangle\}$; the state in question is one of the states $|\psi_i\rangle$ with the probability p_i (> 0). Here the probability p_i satisfies $\sum_i p_i = 1$ and each state $|\psi_i\rangle$ is not necessarily orthogonal to each other but is normalized to one. Then we can describe the state in question by using the density matrix

$$\rho = \sum_i p_i |\psi_i\rangle\langle\psi_i|. \tag{1.2.1}$$

Hereafter, the word "state" refers to a state described by a density matrix unless specified explicitly. When the density matrix of a state has only the probability for an index, that is $p_j = 1$ and $p_i = 0$ $(i \neq j)$, we call the state a pure state. We often refer to a pure state as a wave vector $|\psi_i\rangle$ rather than a density matrix. When more than an index have non-zero probabilities, we call the state a mixed state. We note that a mixed state does not have a corresponding wave vector.

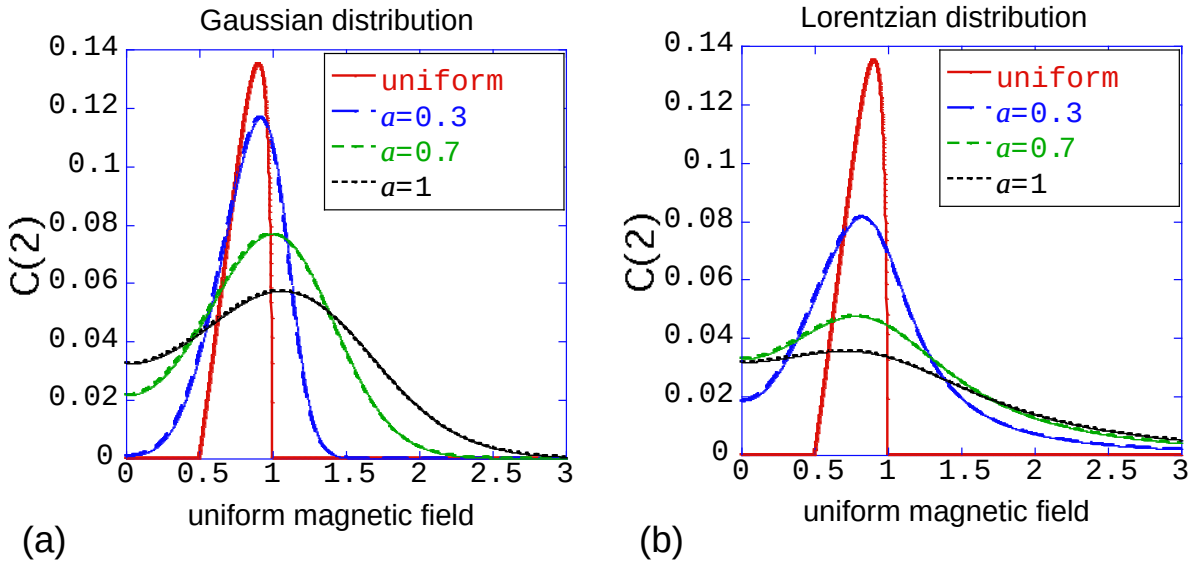

Figure 1.1: (a) The next-nearest-neighbor concurrence of the XY spin chain in the random magnetic field obeying the Gaussian distribution is plotted as a function of the uniform magnetic field. The parameter a denotes the standard deviation of the Gaussian distribution. The red line is the next-nearest-neighbor concurrence in the uniform magnetic field. (b) The next-nearest-neighbor concurrence of the XY spin chain in the random magnetic field obeying the Lorentzian distribution is plotted as a function of a uniform magnetic field. The parameter a denotes the half width at half maximum of the Lorentzian distribution. The red line is the next-nearest-neighbor concurrence in the uniform magnetic field.

To confirm the validity of describing a quantum state with the density matrix, we look into the expectation value of an observable O of the state ρ. We define the expectation value, or the ensemble average of the observable O of ρ as follows:

$$\langle O\rangle = \sum_i p_i \langle\psi_i|O|\psi_i\rangle. \tag{1.2.2}$$

We can obtain the ensemble average (1.2.2) by using the density matrix in the form

$$\mathrm{Tr}(\rho O) = \sum_{i,j} p_i \langle j|\psi_i\rangle\langle\psi_i|O|j\rangle = \sum_i p_i \langle\psi_i|O|\psi_i\rangle, \tag{1.2.3}$$

where $\{|j\rangle\}$ is an orthonormal basis.

We next introduce the density matrix whose system is in equilibrium with a heat bath. Suppose that the state of the system given by the Hamiltonian H is in the ensemble $\{p_i, |\varphi_i\rangle,\ (i = 1, 2, \cdots, n)\}$ and is in equilibrium with the heat bath of the temperature T, where n is the dimension of the system and $|\varphi_i\rangle$ satisfies the eigenequation

$$H|\varphi_i\rangle = E_i|\varphi_i\rangle, \quad (i = 1, 2, \cdots, n) \tag{1.2.4}$$

with E_i the eigenvalue of the eigenstate $|\varphi_i\rangle$. We obtain the density matrix ρ of the equilibrium state of the system by using Eq. (1.2.1) as

$$\rho = \sum_{i=1}^{n} \frac{e^{-\beta E_i}}{Z} |\varphi_i\rangle\langle\varphi_i|, \tag{1.2.5}$$

where we assume that the system obeys the canonical distribution and Z is the partition function of the system,

$$Z = \mathrm{Tr} e^{-\beta H} \tag{1.2.6}$$

with $\beta = (k_B T)^{-1}$. Equation (1.2.4) with the completeness relation is followed by

$$\begin{aligned} \rho &= \sum_{i=1}^{n} \frac{e^{-\beta E_i}}{Z} |\varphi_i\rangle\langle\varphi_i| \\ &= \sum_{i=1}^{n} \frac{e^{-\beta H}}{Z} |\varphi_i\rangle\langle\varphi_i| = \frac{e^{-\beta H}}{Z}. \end{aligned} \tag{1.2.7}$$

We thus obtain the density matrix which often appears in statistical mechanics. The thermal average of an observable O is given by

$$\langle O\rangle_T = \mathrm{Tr}\rho O = \frac{\mathrm{Tr} O e^{-\beta H}}{\mathrm{Tr} e^{-\beta H}} \tag{1.2.8}$$

Next, we see that the density matrix ρ at zero temperature $T = 0$ is reduced to $\rho_0 = |\varphi_0\rangle\langle\varphi_0|$, where $|\varphi_0\rangle$ is the ground state. The limit $\beta \to \infty$ leads to

$$\begin{aligned}\rho_0 &= \lim_{\beta\to\infty} \frac{e^{-\beta H}}{Z} = \lim_{\beta\to\infty} \frac{e^{-\beta E_0}|\varphi_0\rangle\langle\varphi_0| + e^{-\beta E_1}|\varphi_1\rangle\langle\varphi_1| + \cdots e^{-\beta E_n}|\varphi_n\rangle\langle\phi_n|}{e^{-\beta E_0} + e^{-\beta E_1} + \cdots + e^{-\beta E_N}} \\ &= \lim_{\beta\to\infty} \frac{|\varphi_0\rangle\langle\varphi_0| + e^{-\beta(E_1-E_0)}|\varphi_1\rangle\langle\varphi_1| + \cdots + e^{-\beta(E_n-E_0)}|\varphi_n\rangle\langle\varphi_n|}{1 + e^{-\beta(E_1-E_0)} + \cdots + e^{-\beta(E_n-E_0)}} \\ &= |\varphi_0\rangle\langle\varphi_0|, \end{aligned} \tag{1.2.9}$$

where we assume $E_0 < E_1 \leq \cdots \leq E_n$. In the present thesis, the ground-state degeneracy occurs only at limited points with zero measure, and hence we ignore the ground-state degeneracy.

1.2.2 The reduced density matrix

Next, we introduce the reduced density matrix. The reduced density matrix is needed to measure the entanglement between two spins in an N-spin system.

Suppose that Alice and Bob have the physical systems A and B, whose state is described by the density matrix ρ_{AB}. The reduced density matrix for the system A is given by

$$\rho_A = \mathrm{Tr}_B \rho_{AB}, \tag{1.2.10}$$

where Tr_B denotes the trace operation over the degrees of freedom of the system B. The reduced density matrix holds the information of the system A in the sense that it gives us the expectation value of an observable O_A for the system A. We can easily confirm the fact as follows:

$$\mathrm{Tr}\left(\rho_{AB} O_A \otimes I_B\right) = \mathrm{Tr}_A\left[\mathrm{Tr}_B(\rho_{AB} O_A \otimes I_B)\right] = \mathrm{Tr}_A(O_A \rho_A). \tag{1.2.11}$$

We show an example of the reduced density matrix for a two-qubit system. The qubit is a quantum system with two energy levels. We imagine that Alice and Bob share a pair of qubits whose state is the singlet $|\Psi_{AB}\rangle = \frac{1}{\sqrt{2}}(|0_A 1_B\rangle - |1_A 0_B\rangle)$, where the subscript A indicates that the first system belongs to Alice and the subscript B indicates that the second system belongs to Bob. When Alice makes a measurement, the expectation values of the observable $O_A = a|0_A\rangle\langle 0_A| + b|1_A\rangle\langle 1_A|$ with real numbers a and b is

$$\mathrm{Tr}\left(|\Psi_{AB}\rangle\langle\Psi_{AB}| O_A \otimes I_B\right) = \frac{a+b}{2}. \tag{1.2.12}$$

We obtain the same result in terms of the reduced density matrix. We first calculate the reduced density matrix:

$$\begin{aligned}\rho_A &= \mathrm{Tr}_B |\Psi_{AB}\rangle\langle\Psi_{AB}| \\ &= \mathrm{Tr}_B \left[\frac{1}{2}(|0_A 1_B\rangle - |1_A 0_B\rangle)(\langle 0_A 1_B| - \langle 1_A 0_B|)\right] \\ &= \frac{1}{2}\left(|0_A\rangle\langle 0_A| + |1_A\rangle\langle 1_A|\right). \end{aligned} \tag{1.2.13}$$

The density matrix ρ_A describes that the state is the equal mixture of the levels $|0_A\rangle$ and $|1_A\rangle$. By using Eq. (1.2.3), we have the expectation value of the observable O_A as

$$\mathrm{Tr}_A\left(\rho_A O_A\right) = \frac{a+b}{2}. \tag{1.2.14}$$

We thus demonstrated that the reduced density matrix ρ_A holds the information of the system A.

1.2.3 The one-qubit and two-qubit density matrices

Now, we explain a procedure of obtaining a reduced density matrix for a general Hamiltonian. In the present thesis, we need two-qubit density matrices in order to use the concurrence as a measure of the entanglement. We show that one-qubit and two-qubit density matrices can be constructed from one-point and two-point correlation functions.

The one-qubit density matrix is a reduced density matrix given by

$$\rho_i = \mathrm{Tr}_{\hat{i}}\rho, \tag{1.2.15}$$

where $\mathrm{Tr}_{\hat{i}}$ denotes the partial trace over all degrees of freedom except for the ith qubit. The two-qubit density matrix is a reduced density matrix given by

$$\rho_{ij} = \mathrm{Tr}_{\hat{ij}}\rho, \tag{1.2.16}$$

where $\mathrm{tr}_{\hat{ij}}$ denotes the partial trace over all degrees of freedom except for the ith and jth qubits.

Since the one-qubit density matrix is Hermitian, it can be expanded by the Pauli matrices and the identity matrix in the form

$$\rho_i = \mathrm{Tr}_{\hat{i}}\rho = \frac{1}{2}\sum_{\alpha=0}^{3} q_\alpha \sigma_i^\alpha, \tag{1.2.17}$$

where σ_i^0 denotes the identity matrix acting on the ith qubit, σ_i^1, σ_i^2, σ_i^3 are the Pauli matrices σ_i^x, σ_i^y, σ_i^z acting on the ith qubit, and $\{q_\alpha\}$ are real numbers. To construct the density matrix, we evaluate the coefficients q_α. First, as the trace of the density matrix is unity, the coefficient q_0 must be equal to 1. The other coefficients q_α are determined by the relations

$$q_\alpha = \mathrm{tr}_i(\sigma_i^\alpha \rho_i) = \mathrm{tr}_i(\sigma_i^\alpha \mathrm{tr}_{\hat{i}}\rho) = \mathrm{tr}(\sigma_i^\alpha \rho) = \langle \sigma_i^\alpha \rangle \tag{1.2.18}$$

for $\alpha = 1, 2, 3$. We can thus obtain the one-qubit density matrix by calculating the one-point functions.

Similarly, the two-qubit density matrix can be expanded by the tensor product of the Pauli matrices and the identity matrix in the form

$$\rho_{ij} = \mathrm{tr}_{\hat{ij}}(\rho) = \frac{1}{4}\sum_{\alpha,\beta=0}^{3} p_{\alpha\beta}\sigma_i^\alpha \otimes \sigma_j^\beta, \tag{1.2.19}$$

where $p_{\alpha\beta}$ are real numbers because ρ_{ij} is an Hermite matrix. The coefficients $p_{\alpha\beta}$ are determined by the relations

$$p_{\alpha\beta} = \mathrm{tr}_{ij}(\sigma_i^\alpha \sigma_j^\beta \rho_{ij}) = \mathrm{tr}(\sigma_i^\alpha \sigma_j^\beta \rho) = \langle \sigma_i^\alpha \sigma_j^\beta \rangle. \tag{1.2.20}$$

Since the trace of the density matrix is unity, the coefficient p_{00} must be equal to 1. Calculating the two-point functions (1.2.20), we can construct the two-qubit density matrix.

When we construct the density matrix of a particular model (*e.g.* XYmodel), the symmetry of the model often reduces the number of the independent coefficients that we have to calculate. This will be shown in §3.2.

1.3 Definition of an entangled state

1.3.1 Definition of a pure entangled state

In this section, we define an entangled state mathematically. First, we define a pure entangled state. Consider a composite system of the subsystems A and B. A pure entangled state is a state that cannot be written by the tensor product of a pure state $|\psi_A\rangle$ of the subsystem A and a pure state $|\psi_B\rangle$ of the subsystem B:

$$|\Psi_{AB}\rangle \neq |\psi_A\rangle \otimes |\psi_B\rangle. \tag{1.3.1}$$

Conversely, if a state of the composite system of A and B can be written by the tensor product of a pure state $|\psi_A\rangle$ of the subsystem A and a pure state $|\psi_B\rangle$ of the subsystem B, the state is called a separable state. A separable state does not have entanglement.

Typical examples of the pure entangled state are the following states:

$$|\Psi_{AB}^+\rangle = \frac{1}{\sqrt{2}}(|0_A 1_B\rangle + |1_A 0_B\rangle), \tag{1.3.2}$$

$$|\Psi_{AB}^-\rangle = \frac{1}{\sqrt{2}}(|0_A 1_B\rangle - |1_A 0_B\rangle), \tag{1.3.3}$$

$$|\Phi_{AB}^+\rangle = \frac{1}{\sqrt{2}}(|0_A 0_B\rangle + |1_A 1_B\rangle), \tag{1.3.4}$$

and

$$|\Phi_{AB}^-\rangle = \frac{1}{\sqrt{2}}(|0_A 0_B\rangle - |1_A 1_B\rangle). \tag{1.3.5}$$

These states are known as the Bell states or the EPR states. The states (1.3.2)–(1.3.5) are the orthonormal bases of the system consisting of two qubits. Each Bell state is the superposition of two states having the same amplitude $1/\sqrt{2}$. We refer to such a state as a maximally entangled state. On the other hand, a partially entangled state is a state which cannot be written by the tensor product of a pure state and is the superposition of two states not having the same amplitude.

1.3.2 Definition of a mixed entangled state

Here we define a mixed entangled state mathematically. For this purpose, we first mention ambiguity of the expansion of a mixed state. A mixed state is an ensemble of pure states and is represented only in terms of the density matrix (1.2.1). Suppose that the mixed state ρ is given in the form

$$\rho = \frac{1}{2}|\Phi^+_{AB}\rangle\langle\Phi^+_{AB}| + \frac{1}{2}|\Phi^-_{AB}\rangle\langle\Phi^-_{AB}|, \tag{1.3.6}$$

where $|\Phi^\pm_{AB}\rangle = \frac{1}{\sqrt{2}}(|0_A 0_B\rangle \pm |1_A 1_B\rangle)$. The state ρ seems to be an equal mixture of the maximally entangled states $|\Phi^+_{AB}\rangle$ and $|\Phi^-_{AB}\rangle$. The state ρ, however, can also be written in the form

$$\rho = \frac{1}{2}|0_A 0_B\rangle\langle 0_A 0_B| + \frac{1}{2}|1_A 1_B\rangle\langle 1_A 1_B|. \tag{1.3.7}$$

The state ρ now seems to be an equal mixture of the separable states $|0_A 0_B\rangle$ and $|1_A 1_B\rangle$. Any measurements on ρ can be explained in terms of the separable states.

Thus we define the mixed entangled state of a composite system of A and B in the following way: A mixed state ρ_{AB} is entangled if and only if *for any representations* of ρ_{AB}, it cannot be written as

$$\rho_{AB} \neq \sum_i p_i \rho^A_i \otimes \rho^B_i, \tag{1.3.8}$$

where ρ^A_i is a pure state of the subsystem A, ρ^B_i is a pure state of the subsystem B and $\sum_i p_i = 1$. This is the definition of a mixed entangled state.

1.4 Quantum teleportation

In this section, we review an application of entangled states, namely the quantum teleportation [1], where the entanglement plays a key role. We imagine the situation that Alice wants to deliver the state $|\psi_A\rangle = \alpha|0_A\rangle + \beta|1_A\rangle$ to Bob, or to have Bob make a copy of the state, $|\psi_B\rangle = \alpha|0_B\rangle + \beta|1_B\rangle$, but Alice does not know the values α and β. Moreover, Alice is allowed to use only classical communications (*e.g.* a telephone) and to operate only on her system. This situation is often referred to as the local operation and classical communication, or LOCC. Alice, however, can deliver the state $|\psi_A\rangle$ to Bob by using an entangled state shared by Alice and Bob as follows. Suppose that Alice and Bob share the entangled state

$$|\Psi^+_{A'B}\rangle = \frac{1}{\sqrt{2}}(|0_{A'} 0_B\rangle + |1_{A'} 1_B\rangle), \tag{1.4.1}$$

where $|0_{A'}\rangle$ and $|1_{A'}\rangle$ are the states of another qubit belonging to Alice. First, Alice makes the tensor product

$$\begin{aligned}|\psi_0\rangle = |\psi_A\rangle \otimes |\Psi^+_{A'B}\rangle &= \frac{1}{\sqrt{2}}(\alpha|0_A\rangle + \beta|1_A\rangle) \otimes (|0_{A'}0_B\rangle + |1_{A'}1_B\rangle) \\ &= \frac{1}{\sqrt{2}}\left[\alpha|0_A\rangle(|0_{A'}0_B\rangle + |1_{A'}1_B\rangle) + \beta|1_A\rangle(|0_{A'}0_B\rangle + |1_{A'}1_B\rangle)\right],\end{aligned} \tag{1.4.2}$$

where the first two qubits A and A' belong to Alice and the third qubit B belongs to Bob. Next, Alice operates on the first two qubits of the state $|\psi_0\rangle$ a unitary operator called the controlled-NOT gate

$$U_{\text{c-NOT}} = |0_A0_{A'}\rangle\langle 0_{A'}0_A| + |0_A1_{A'}\rangle\langle 1_{A'}0_A| + |1_A0_{A'}\rangle\langle 1_{A'}1_A| + |1_A1_{A'}\rangle\langle 0_{A'}1_A|. \tag{1.4.3}$$

Then she has the state

$$|\psi_1\rangle = U_{\text{c-NOT}}|\psi_0\rangle = \frac{1}{\sqrt{2}}\left[\alpha|0_A\rangle(|0_{A'}0_B\rangle + |1_{A'}1_B\rangle) + \beta|1_A\rangle(|1_{A'}0_B\rangle + |0_{A'}1_B\rangle)\right]. \tag{1.4.4}$$

Next, she operates on the first qubit A of the state $|\psi_1\rangle$ another unitary operator called the Hadamard gate

$$U_{\text{H}} = \frac{1}{\sqrt{2}}\left(|0_A\rangle\langle 0_A| + |0_A\rangle\langle 1_A| + |1_A\rangle\langle 0_A| - |1_A\rangle\langle 1_A|\right). \tag{1.4.5}$$

Then she obtains the state

$$\begin{aligned}|\psi_2\rangle &= U_{\text{H}}|\psi_1\rangle \\ &= \frac{1}{2}\left[\alpha(|0_A\rangle + |1_A\rangle)(|0_{A'}0_B\rangle + |1_{A'}1_B\rangle) + \beta(|0_A\rangle - |1_A\rangle)(|1_{A'}0_B\rangle + |0_{A'}1_B\rangle)\right] \\ &= \frac{1}{2}\big[|0_A0_{A'}\rangle(\alpha|0_B\rangle + \beta|1_B\rangle) + |1_A0_{A'}\rangle(\alpha|0_B\rangle + \beta|1_B\rangle) \\ &\quad + |1_A0_{A'}\rangle(\alpha|0_B\rangle - \beta|1_B\rangle) + |1_A1_{A'}\rangle(\alpha|0_B\rangle - \beta|1_B\rangle)\big].\end{aligned} \tag{1.4.6}$$

If Alice performs a measurement on the first two qubits A and A', the possible outcomes of Alice's measurement are

$$|0_A0_{A'}\rangle \mapsto \alpha|0_B\rangle + \beta|1_B\rangle, \tag{1.4.7}$$
$$|0_A1_{A'}\rangle \mapsto \alpha|1_B\rangle + \beta|0_B\rangle, \tag{1.4.8}$$
$$|1_A0_{A'}\rangle \mapsto \alpha|0_B\rangle - \beta|1_B\rangle, \tag{1.4.9}$$
$$|1_A1_{A'}\rangle \mapsto \alpha|1_B\rangle + \beta|0_B\rangle, \tag{1.4.10}$$

where the left-hand sides denote the outcome of Alice's measurement and the right-hand sides denote Bob's state after Alice's measurement. Depending on the outcome of Alice's

measurement, Bob's qubit becomes one of these four states. If Alice's outcome is $|0_A 0_{A'}\rangle$, she tells Bob by using classical communication not to do any operation. If Alice's outcome is $|0_A 1_{A'}\rangle$, she tells Bob to apply the unitary transformation $|0_B\rangle\langle 0_B| - |1_B\rangle\langle 0_1|$ so that he can get the state $|\psi_B\rangle = \alpha|0_B\rangle + \beta|1_B\rangle$. If Alice measures the other outcomes, Bob's appropriate unitary transformation again leads Bob to get the state $|\psi_B\rangle$. This procedure is called the quantum teleportation. The quantum teleportation has been experimentally realized in various forms [13–16].

We note that when the quantum teleportation is completed, Alice loses the state $|\psi_A\rangle$. Note also that the quantum teleportation cannot deliver information faster than the light because Alice and Bob use classical communications.

Chapter 2

The von Neumann entropy and the entanglement of formation

In this chapter, we review how the entanglement is quantified [17–21]. Here, LOCC, where only use of local operation and classical communication are allowed, is a key concept to quantify it. Suppose that in a bipartite system with the subsystems A and B, Alice can only operate on the subsystem A, Bob can only operate on the subsystem B, and they can communicate the results of their measurements only through classical ways of communication (*e.g.* Alice telephones Bob). This is an example of LOCC.

If we were allowed to use quantum operations on the subsystems A and B, we could always create a maximally entangled state, namely one of the Bell states (1.3.2)–(1.3.5), from a completely disentangled state. To quantify the entanglement, we hence are allowed to use LOCC only; LOCC is also used in quantum information processing, such as quantum teleportation as seen in §1.4.

The von Neumann entropy is a measure of the entanglement of a pure state of a bipartite system. It cannot be used for measuring entanglement of a mixed state. We therefore use the entanglement of formation as a measure of entanglement of a mixed state.

In the following sections, we review the von Neumann entropy for a pure state and the entanglement of formation for a mixed state; we quantify entanglement by measuring the efficiency with which we can convert a Bell state into the state in question.

2.1 The von Neumann entropy

In this section, we introduce the von Neumann entropy and explain why it can measure the entanglement of a pure state of a bipartite system. For a pure state of any bipartite systems with the subsystems A and B, the von Neumann entropy is given by

$$S(\rho) = -\mathrm{Tr}(\rho_A \log_2 \rho_A) = -\mathrm{Tr}(\rho_B \log_2 \rho_B), \tag{2.1.1}$$

where ρ_A and ρ_B are reduced density matrices. Note that unlike the von Neumann entropy in statistical mechanics, the logarithms are taken in base two. It is easy to confirm the

equality

$$-\mathrm{Tr}(\rho_A \log_2 \rho_A) = -\mathrm{Tr}(\rho_B \log_2 \rho_B) \tag{2.1.2}$$

by the Schmidt decomposition (see Appendix A). From now on, $S(|\psi\rangle)$ denotes $S(|\psi\rangle\langle\psi|)$ for a pure state $|\psi\rangle$. (Note that for a mixed state ρ, we cannot write $S(\rho)$ as $S(|\psi\rangle)$, since the mixed state ρ does not have a corresponding wave vector $|\psi\rangle$.) When the system of the Hamiltonian is given by a tensor product $\mathbb{C}^N \otimes \mathbb{C}^N$, for example, the von Neumann entropy takes the value from 0 for a separable state to $\log_2 N$ for a maximally entangled state.

Now, we explain why the von Neumann entropy can measure entanglement of a pure state. It is based on the efficiency of converting a Bell state into another state [17].

Suppose that Alice and Bob have a certain number of copies of the singlet $|\Phi\rangle = \frac{1}{\sqrt{2}}(|0_A 1_B\rangle - |1_A 0_B\rangle)$ and then from them create n copies of a pure state $|\phi\rangle = \sqrt{p}|0_A 0_B\rangle + \sqrt{1-p}|1_A 1_B\rangle$ by using LOCC only. Here we note that thanks to the Schmidt decomposition, any two-qubit states can be written in the form $|\phi\rangle = \sqrt{p}|0_A 0_B\rangle + \sqrt{1-p}|1_A 1_B\rangle$ (see Appendix A).

It is known that $nS(|\phi\rangle)$ copies of the singlet $|\Phi\rangle$ are needed to produce n copies of the state $|\phi\rangle$ for large n, where $S(|\phi\rangle)$ is the von Neumann entropy

$$S(|\phi\rangle) = -\mathrm{Tr}\rho_A \log_2 \rho_A = -p \log_2 p - (1-p)\log_2(1-p) \tag{2.1.3}$$

with ρ_A the reduced density matrix

$$\rho_A = p|0_A\rangle\langle 0_A| + (1-p)|1_A\rangle\langle 1_A|; \tag{2.1.4}$$

see Fig. 2.1.

The procedure of creating $|\phi\rangle^{\otimes n}$ from a certain number of copies of the singlet $|\Phi\rangle$ by LOCC is called the entanglement dilution. Conversely, they need n copies of $|\phi\rangle$ in order to obtain $nS(|\phi\rangle)$ copies of the singlet $|\Phi\rangle$ by LOCC. This procedure of creating $|\Phi\rangle^{\otimes nS(|\phi\rangle)}$ from $|\phi\rangle^{\otimes n}$ is called the entanglement concentration. For any pure state $|\phi\rangle$, the entanglement dilution and concentration are reversible processes:

$$|\Phi\rangle^{\otimes nS(|\phi\rangle)} \rightleftarrows |\phi\rangle^{\otimes n} \tag{2.1.5}$$

The von Neumann entropy S tells us with what efficiency they can make a pure state $|\phi\rangle$ from a Bell state and conversely, with what efficiency they can make a Bell state from a state $|\phi\rangle$. We may then interpret the efficiency as how close the state $|\phi\rangle$ is to a maximally entangled Bell state. We hence regard the von Neumann entropy as a measure of entanglement of the pure state $|\phi\rangle$.

2.2 The entanglement of formation

In this section, we introduce the entanglement of formation and why it can measure the entanglement of a mixed state of a bipartite system. For a mixed state ρ of the bipartite

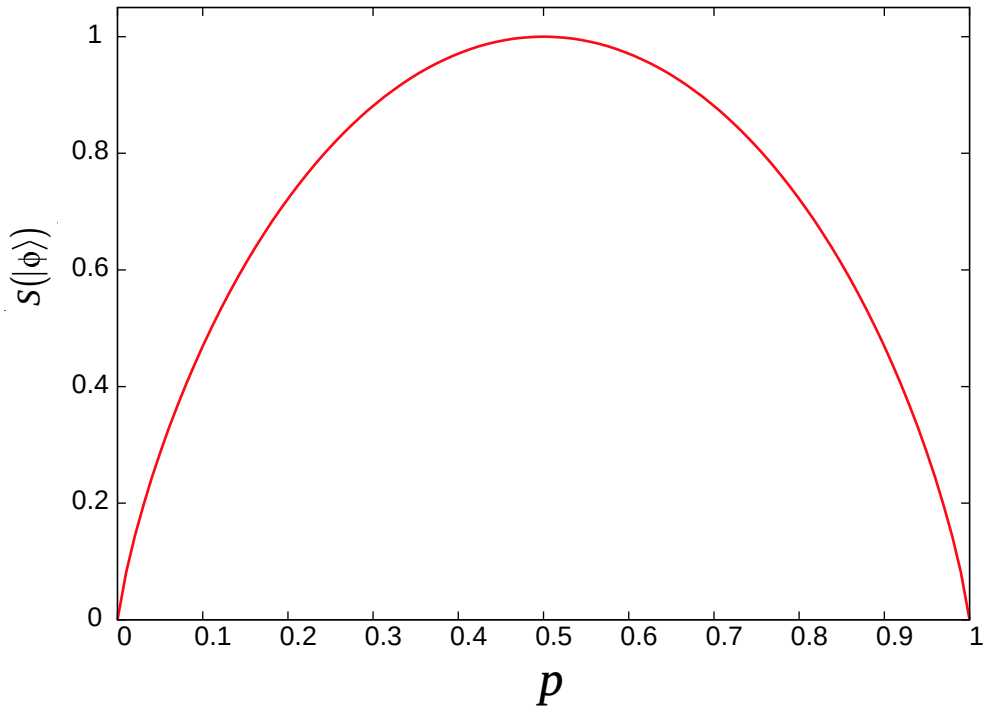

Figure 2.1: The von Neumann entropy of the state $|\phi\rangle = \sqrt{p}|0_A 0_B\rangle + \sqrt{1-p}|1_A 1_B\rangle$.

system, the entanglement of formation [19] is given by

$$E(\rho) = \inf_{\{p_i, |\psi_i\rangle\}} \sum_i p_i S(|\psi_i\rangle), \tag{2.2.1}$$

where $S(|\psi_i\rangle)$ is the von Neumann entropy and the infimum is taken over all the ways of the decomposition $\rho = \sum_i p_i |\psi_i\rangle\langle\psi_i|$; note that there can be many ways of expression of a mixed state in the form $\rho = \sum_i p_i |\psi_i\rangle\langle\psi_i|$. We immediately confirm that if a density matrix ρ represents a pure state $|\psi_i\rangle$, the entanglement of formation $E(\rho)$ is reduced to the von Neumann entropy $S(|\psi_i\rangle)$.

We cannot use the von Neumann entropy to measure the entanglement of a mixed state, because a mixed state can have a finite von Neumann entropy even if there is no entanglement. Consider the mixed state

$$\sigma = \frac{1}{2}|\Phi^+\rangle\langle\Phi^+| + \frac{1}{2}|\Phi^-\rangle\langle\Phi^-| \tag{2.2.2}$$

with $|\Phi^\pm\rangle = \frac{1}{\sqrt{2}}(|0_A 0_B\rangle \pm |1_A 1_B\rangle)$. This state is an ensemble of equal mixture of the maximally entangled states $|\Phi^+\rangle$ and $|\Phi^-\rangle$. The state (2.2.2) is in fact not entangled because it can be rewritten as a separable state of the form

$$\sigma = \frac{1}{2}|0_A 0_B\rangle\langle 0_A 0_B| + \frac{1}{2}|1_A 1_B\rangle\langle 1_A 1_B|. \tag{2.2.3}$$

However, the von Neumann entropy of the state σ gives $S(\sigma_A) = S(\sigma_B) = 1$. Hence, the entanglement of a mixed state cannot be quantified by the von Neumann entropy.

The entanglement of formation (2.2.1) is a generalization of the von Neumann entropy. Suppose that Alice and Bob have a certain number of copies of the singlet and create n copies of a mixed state ρ for large n from them by LOCC only. We consider how many singlets they need to make $\rho^{\otimes n}$. Suppose that a representation of the mixed state ρ is given in the form

$$\rho = \sum_{i=1}^{M} p_i |\psi_i\rangle\langle\psi_i|, \tag{2.2.4}$$

where $|\psi_i\rangle$ is a pure state and not necessarily orthogonal to each other. The n copies of the state ρ may be considered to contain np_i copies of the pure state $|\psi_i\rangle$. To produce np_1 copies of $|\psi_1\rangle$ through the entanglement dilution, they need $np_1 S(|\psi_1\rangle)$ copies of the singlet for large n as before (see the previous section). Similarly, the other states $|\psi_i\rangle$ $(i = 2, \cdots, M)$ are also created out of $np_i S(|\psi_i\rangle))$ copies of the singlet for large n, respectively. They collect all the copies into a large ensemble. Finally, they discard any records indicating which singlets generate each $|\psi_i\rangle$; if they did not discard the records, the assembled states would not be mixed stochastically and hence would not be described in the form Eq. (2.2.4).

The total number of the singlets they used is

$$n \sum_{i=1}^{M} p_i S(|\phi_i\rangle). \tag{2.2.5}$$

Equation (2.2.5) divided by n may be an entanglement measure. The mixed state ρ, however, has many representations of the form (2.2.4). We adopt the minimum number and hence define the entanglement of formation as in Eq. (2.2.1). We thus have

$$|\Phi\rangle^{\otimes nE(\rho)} \longrightarrow \rho^{\otimes n}, \tag{2.2.6}$$

for large n. (There is actually a more efficient procedure of the entanglement dilution of a mixed state, but we do not go into it in the present thesis.)

Unlike for the pure states, the entanglement dilution and the entanglement concentration are not reversible for mixed states. Suppose that Alice and Bob manage to concentrate n copies of a mixed state ρ with large n into $nE_D(\rho)$ copies of the Bell state $|\Phi\rangle$ as in

$$\rho^{\otimes n} \longrightarrow |\Phi\rangle^{\otimes nE_D(\rho)},$$

where E_D is called the distillable entanglement. It has been proved [18, 19] that the entanglement of formation $E(\rho)$ is greater than the distillable entanglement $E_D(\rho)$ for any mixed states:

$$E(\rho) > E_D(\rho). \tag{2.2.7}$$

Thus the procedures of the entanglement dilution and concentration for a mixed state are irreversible:

$$|\Phi\rangle^{\otimes nE} \longrightarrow \rho^{\otimes n} \longrightarrow |\Phi\rangle^{\otimes nE_D}, \quad (nE_D < nE). \tag{2.2.8}$$

We could regard both E and E_D as measures of the entanglement. However, the distillable entanglement can be zero even if the state is nonseparable. In contrast, the entanglement of formation of a state ρ is zero if and only if ρ is separable. We thus use the entanglement of formation as a measure of entanglement in the present thesis.

Finally, we introduce Wootters' formula [22], which enables us to calculate the entanglement of formation of a two-qubit system. Wootters' formula tells us that for a density matrix ρ of a two-qubit system, the entanglement of formation is given by the formula

$$E(\rho) = h\left(\frac{1+\sqrt{1-C(\rho)^2}}{2}\right), \tag{2.2.9}$$

where

$$h(x) = -x\log_2 x - (1-x)\log_2(1-x) \tag{2.2.10}$$

and $C(\rho)$ is called the concurrence given by

$$C(\rho) = \max\{0, \lambda_1 - \lambda_2 - \lambda_3 - \lambda_4\}. \tag{2.2.11}$$

Here, $\{\lambda_i\}$ are the square roots of the eigenvalues of the matrix $R = \rho\tilde{\rho}$ in the descending order, $\lambda_1 \geq \lambda_2 \geq \lambda_3 \geq \lambda_4$, where $\tilde{\rho} = (\sigma^y \otimes \sigma^y)\rho^*(\sigma^y \otimes \sigma^y)$. Note that the complex conjugate ρ^* is taken in the σ^z bases, $|\uparrow\rangle$ and $|\downarrow\rangle$. Even though the matrix $R = \rho\tilde{\rho}$ is not necessarily a Hermite matrix, all the eigenvalues of R are non-negative, because ρ and $\tilde{\rho}$ are positive definite matrices. We can regard the concurrence (2.2.11) as an entanglement measure, because the entanglement of formation (2.2.9) is a monotonically increasing function of the concurrence; see Fig. 2.2.

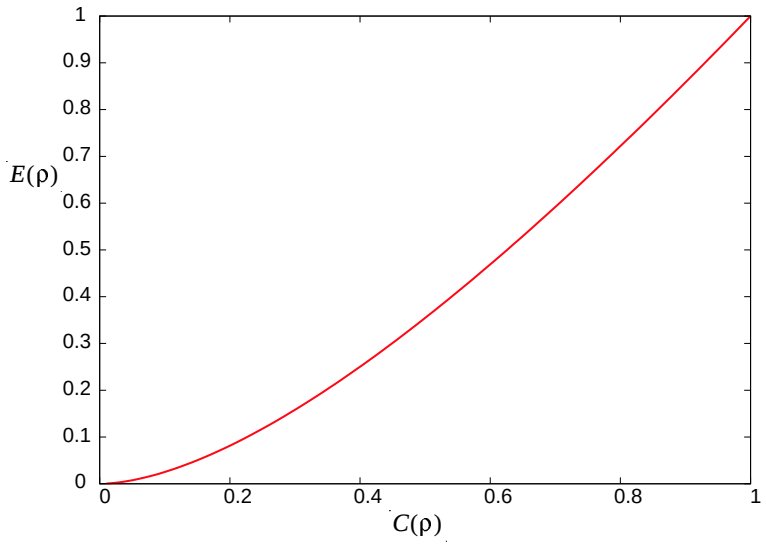

Figure 2.2: The entanglement of formation as a function of the concurrence. It is a monotonically increasing function of the concurrence as in Eq. (2.2.9).

Chapter 3

The entanglement of the XY spin chain in a random magnetic field

In this chapter, we numerically measure the entanglement of the XY spin chain in a random magnetic field using the concurrence and study how the randomness influences the entanglement.

This chapter is arranged as follows. We first introduce the model. Next, we show how to construct the two-qubit density matrix. Next, we calculate the one-point and two-point correlations in order to construct the reduced density matrix. Finally, we study the behavior of the concurrence.

3.1 XY model in a random magnetic field

The model that we consider here is given by the Hamiltonian

$$H = -J\sum_{j=1}^{N}(S_j^x S_{j+1}^x + S_j^y S_{j+1}^y) - \sum_{j=1}^{N}(h + h_j)S_j^z, \tag{3.1.1}$$

where $S^\alpha = \frac{1}{2}\sigma^\alpha$ $(\alpha = x, y, z)$ with σ^α being the Pauli matrices,

$$\sigma^x = \begin{pmatrix} 0 & 1 \\ 1 & 0 \end{pmatrix}, \quad \sigma^y = \begin{pmatrix} 0 & -i \\ i & 0 \end{pmatrix}, \quad \sigma^z = \begin{pmatrix} 1 & 0 \\ 0 & -1 \end{pmatrix},$$

N is the number of the spins, J (> 0) is the exchange coupling constant, h is a uniform magnetic field and h_j is a random magnetic field. We here impose the periodic boundary conditions

$$S_{N+j}^\alpha = S_j^\alpha \quad (\alpha = x, y, z). \tag{3.1.2}$$

The probability distribution of the random magnetic field h_j is given by

$$P_q(h_j) = A_{q,a}[a^2 - (1-q){h_j}^2]^{\frac{1}{1-q}}, \tag{3.1.3}$$

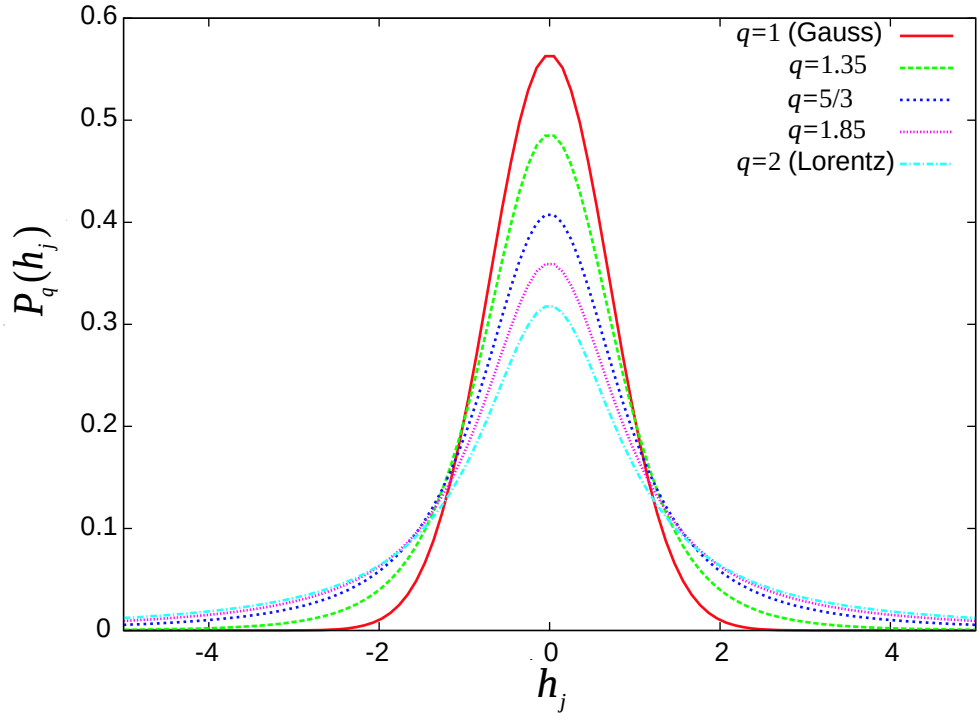

Figure 3.1: The probability distribution (3.1.3) gives a Gaussian distribution function for $q = 1$ with a equal to its standard deviation σ, while it gives a Lorentzian distribution function for $q = 2$ with a equal to its half width at half maximum. The figure is drawn for $a = 1$ for all cases.

where a is a scale parameter, $A_{q,a}$ is the normalization constant and q is a real number that determines the type of the distribution. Each h_j is independent of the other sites. Equation (3.1.3) is reduced to a Gaussian distribution for $q = 1$ and to a Lorentzian distribution for $q = 2$; see Fig. 3.1. In the case of $q = 1$ (a Gaussian distribution), the scale parameter a gives its standard deviation. In the case of $q = 2$ (a Lorentzian distribution), the scale parameter a gives its half width at half maximum.

In the present thesis, we study the cases $q = 1$, 1.35, 5/3, 1.85 and 2. The former two cases have finite variance and the latter three cases have infinite variance. The variance of the distribution diverges for $q \geq 5/3$, whereas it is finite for $q < 5/3$. The probability distribution (3.1.3) behaves as $h_j^{2/(1-q)}$ for large h_j and thus we have

$$\langle h_j^2 \rangle \sim \int \mathrm{d}h_j \, h_j^2 h_j^{\frac{2}{1-q}} \sim h_j^{\frac{5-3q}{1-q}}. \tag{3.1.4}$$

We conclude that the variance diverges for

$$\frac{5-3q}{1-q} \geq 0, \tag{3.1.5}$$

or $q \geq 5/3$.

We rewrite Eq. (3.1.1) by using the Jordan-Wigner transformation [27] for later convenience. The Jordan-Wigner transformation maps the spin space into the fermionic space in the form

$$\begin{aligned} S_j^+ &= \prod_{l=1}^{j-1} \exp(-i\pi a_l^\dagger a_l) a_j^\dagger, \\ S_j^- &= \prod_{l=1}^{j-1} \exp(i\pi a_l^\dagger a_l) a_j, \\ S_j^z &= S_j^+ S_j^- - \frac{1}{2} = a_j^\dagger a_j - \frac{1}{2}, \end{aligned} \tag{3.1.6}$$

where $a_i^\dagger$ and a_i are the creation and annihilation operators satisfying the anti-commutation relations $\{a_i^\dagger, a_j\} = \delta_{ij}$ and $\{a_i, a_j\} = 0$. Using the Jordan-Wigner transformation (3.1.6), we have

$$H = -\frac{J}{2} \sum_{j=1}^{N} (a_j^\dagger a_{j+1} + a_{j+1}^\dagger a_j) - \sum_{j=1}^{N} (h + h_j) \left(a_j^\dagger a_j - \frac{1}{2} \right). \tag{3.1.7}$$

The periodic boundary conditions Eq. (3.1.2) in the spin space is transformed to

$$\begin{aligned} a_{N+1} = -a_1,\ a_{N+1}^\dagger = -a_1^\dagger \quad &\text{for even } N_F, \\ a_{N+1} = a_1,\ a_{N+1}^\dagger = a_1^\dagger \quad &\text{for odd } N_F, \end{aligned} \tag{3.1.8}$$

where N_F is the number of the fermions.

3.2 The density matrix of the XY model in a random magnetic field

In this section, we consider what quantities are needed to construct the density matrix of the model (3.1.1). We here use the results in §1.2.3. We focus our interest on the entanglement between two spins.

3.2.1 The density matrix

We first remind readers that the two-qubit density matrix can be expanded by the tensor product of the Pauli matrices and the identity matrix as in Eq. (1.2.19):

$$\rho_{ij} = \mathrm{tr}_{\hat{ij}}(\rho) = \frac{1}{4} \sum_{\alpha,\beta=0}^{3} p_{\alpha\beta} \sigma_i^\alpha \otimes \sigma_j^\beta, \tag{3.2.1}$$

where σ_i^0 is the identity operator I_i on the site i, σ_i^α ($\alpha = 1, 2, 3$) are the Pauli matrices on the site i,

$$\sigma_i^1 = \begin{pmatrix} 0 & 1 \\ 1 & 0 \end{pmatrix}, \quad \sigma_i^2 = \begin{pmatrix} 0 & -i \\ i & 0 \end{pmatrix}, \quad \sigma_i^3 = \begin{pmatrix} 1 & 0 \\ 0 & -1 \end{pmatrix},$$

and the coefficients $\{p_{\alpha\beta}\}$ are determined by the relation (1.2.20):

$$p_{\alpha\beta} = \mathrm{tr}_{ij}(\sigma_i^\alpha \sigma_j^\beta \rho_{ij}) = \mathrm{tr}(\sigma_i^\alpha \sigma_j^\beta \rho) = \langle \sigma_i^\alpha \sigma_j^\beta \rangle. \tag{3.2.2}$$

Noting that $p_{00} = 1$, we have to calculate $4 \times 4 - 1 = 15$ coefficients to construct a two-qubit density matrix.

The number of the independent coefficients is reduced to four thanks to the symmetry of the Hamiltonian. First, the XY Hamiltonian possesses the rotational symmetry about the z-axis; namely the unitary matrix

$$U_{\frac{\pi}{2}} = \prod_{j=1}^{N} \exp(-i\frac{\pi}{4}\sigma_j^z) \tag{3.2.3}$$

satisfies

$$[H, U_{\frac{\pi}{2}}] = 0. \tag{3.2.4}$$

We hence have $[U_{\frac{\pi}{2}}, \rho] = 0$ and, therefore, $\langle \sigma_i^x \sigma_j^x \rangle = \langle \sigma_i^y \sigma_j^y \rangle$:

$$\begin{aligned} \langle \sigma_i^x \sigma_j^x \rangle &= \mathrm{Tr}(\sigma_i^x \sigma_j^x \rho) = \mathrm{Tr}(U_{\frac{\pi}{2}}^{-1} \sigma_i^x U_{\frac{\pi}{2}} U_{\frac{\pi}{2}}^{-1} \sigma_j^x \rho U_{\frac{\pi}{2}}) \\ &= \mathrm{Tr}(U_{\frac{\pi}{2}}^{-1} \sigma_i^x U_{\frac{\pi}{2}} U_{\frac{\pi}{2}}^{-1} \sigma_j^x U_{\frac{\pi}{2}} \rho) = \langle \sigma_i^y \sigma_j^y \rangle. \end{aligned} \tag{3.2.5}$$

Next, the Hamiltonian also possesses the global phase-flip symmetry:

$$U_{\mathrm{flip}} = \prod_{j=1}^{N} \sigma_j^z. \tag{3.2.6}$$

Therefore, two-point correlation functions containing an odd number of σ^x or σ^y vanish; for example,

$$\begin{aligned} \langle \sigma_i^z \sigma_j^x \rangle &= \mathrm{Tr}(\sigma_i^z \sigma_j^x \rho) = \mathrm{Tr}(U_{\mathrm{flip}}^{-1} \sigma_i^z \sigma_j^x \rho U_{\mathrm{flip}}) \\ &= \mathrm{Tr}(\sigma_i^z U_{\mathrm{flip}}^{-1} \sigma_j^x U_{\mathrm{flip}} \rho) = \mathrm{Tr}(\sigma_i^z (-\sigma_j^x) \rho) = -\langle \sigma_i^z \sigma_j^x \rangle = 0, \end{aligned} \tag{3.2.7}$$

and

$$\begin{aligned} \langle \sigma_i^x \rangle &= \mathrm{Tr}(\sigma_i^x \rho) = \mathrm{Tr}(U_{\mathrm{flip}}^{-1} \sigma_i^x \rho U_{\mathrm{flip}}) \\ &= \mathrm{Tr}(U_{\mathrm{flip}}^{-1} \sigma_i^x \rho U_{\mathrm{flip}}) = -\mathrm{Tr}(\sigma_i^x \rho) = -\langle \sigma_i^x \rangle = 0. \end{aligned} \tag{3.2.8}$$

Second, the Hamiltonian is a real matrix in the σ^z bases, so that $\rho_{ij}^* = \rho_{ij}$. Noting that only the elements in σ_j^y are imaginary, we find $\langle \sigma_i^x \sigma_j^y \rangle = \langle \sigma_i^y \sigma_j^x \rangle = 0$.

Hence, the two-qubit density matrices take the form

$$\rho_{ij} = \frac{1}{4}\left(I_{ij} + \langle\sigma_i^z\rangle\sigma_i^z \otimes I_j + \langle\sigma_j^z\rangle I_i \otimes \sigma_j^z + \sum_{\alpha=x,y,z} \langle\sigma_i^\alpha\sigma_j^\alpha\rangle\sigma_i^\alpha \otimes \sigma_j^\alpha \right), \tag{3.2.9}$$

where we note Eq. (3.2.5). Therefore, $\langle\sigma_i^z\rangle, \langle\sigma_j^z\rangle$ and $\langle\sigma_i^\alpha\sigma_j^\alpha\rangle$ ($\alpha = x, z$) are required to determine the density matrices of the model; the number of the independent coefficients are thus reduced to four.

3.2.2 Exact solution of the XY model in uniform field

We first briefly review the solution in a uniform field; that is, $h_i = 0$ for all i [23–25]. Here we only outline the procedure and write down the results. See Appendix B for details.

The Hamiltonian with a uniform magnetic field is given by

$$H = -\frac{J}{2}\sum_{j=1}^{N}(a_j^\dagger a_{j+1} + a_{j+1}^\dagger a_j) - h\sum_{j=1}^{N}\left(a_j^\dagger a_j - \frac{1}{2}\right). \tag{3.2.10}$$

Because of the translational invariance, we use the Fourier transform to diagonalize the Hamiltonian (3.2.10):

$$\begin{aligned} a_j &= \frac{1}{\sqrt{N}}\sum_k e^{ikj}c_k, \\ a_j^\dagger &= \frac{1}{\sqrt{N}}\sum_k e^{-ikj}c_k^\dagger, \end{aligned} \tag{3.2.11}$$

where the wave number k takes the values in Eq. (B.1.22) (see Appendix B). The Hamiltonian (3.2.10) is transformed to

$$H = -\sum_k (J\cos k + h)c_k^\dagger c_k + \frac{Nh}{2}, \tag{3.2.12}$$

where $c_k^\dagger$ and c_k are the creation and annihilation operators satisfying the anti-commutation relations $\{c_k^\dagger, c_{k'}\} = \delta_{kk'}$ and $\{c_k, c_{k'}\} = 0$.

Now that the Hamiltonian has been diagonalized, we are in the position of calculating the one-point and two-point correlation functions. We summarize the results here. In the thermodynamic limit $N \to \infty$, the wave number k becomes continuous. The one-point function $\langle\sigma^z\rangle_T$ at a temperature T is given by

$$\langle\sigma^z\rangle_T = -1 + \frac{2}{\pi}\int_0^\pi \frac{\mathrm{d}\phi}{1 + \exp\left[\beta(J\cos\phi + h)\right]}, \tag{3.2.13}$$

where $\beta = 1/k_B T$. The magnetization in the z direction as a function of a uniform magnetic field is plotted in Fig. 3.2. Hereafter the coupling constant J is set to one in all figures

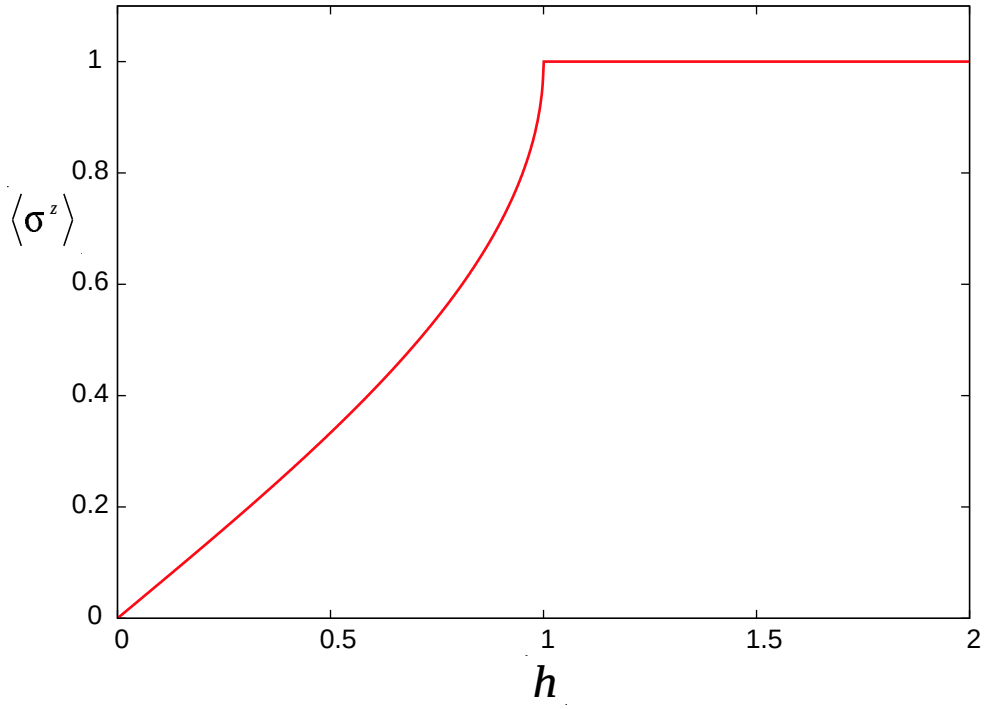

Figure 3.2: The magnetization in the z direction at zero temperature $T = 0$ as a function of the uniform field h, where the coupling constant J is set to one. The quantum phase transition occurs at the point $h = 1$, where the derivative of the $\langle \sigma^z \rangle$ diverges.

in the present thesis. The two-point correlation functions $\langle \sigma_i^\alpha \sigma_j^\alpha \rangle$, $(i < j,\ \alpha = x, y, z)$ are

given in the form

$$\langle\sigma_i^x\sigma_j^x\rangle_T = \begin{vmatrix} G_{i,i+1} & G_{i,i+2} & \cdots & G_{i,j} \\ G_{i+1,i+1} & G_{i+1,i+2} & \cdots & G_{i+1,j} \\ \vdots & \vdots & \ddots & \vdots \\ G_{j-1,i+1} & G_{j-1,i+2} & \cdots & G_{j-1,j} \end{vmatrix}, \tag{3.2.14}$$

$$\langle\sigma_i^y\sigma_j^y\rangle_T = \begin{vmatrix} G_{i+1,i} & G_{i+2,i} & \cdots & G_{j,i} \\ G_{i+1,i+1} & G_{i+2,i+1} & \cdots & G_{j,i+1} \\ \vdots & \vdots & \ddots & \vdots \\ G_{i+1,j-1} & G_{i+2,j-1} & \cdots & G_{j,j-1} \end{vmatrix}, \tag{3.2.15}$$

$$\langle\sigma_i^z\sigma_j^z\rangle_T = \begin{vmatrix} G_{i,i} & G_{i,j} \\ G_{j,i} & G_{j,j} \end{vmatrix}, \tag{3.2.16}$$

where $G_{l,l}$ is

$$G_{l,l} = -1 + \frac{2}{\pi}\int_0^\pi \frac{\mathrm{d}\phi}{1+\exp(-\beta(J\cos\phi + h))}, \tag{3.2.17}$$

and $G_{l,m}$ $(l \neq m)$ is

$$G_{l,m} = \frac{2}{\pi}\int_0^\pi \mathrm{d}\phi \frac{\cos(l-m)\phi}{1+\exp(-\beta(J\cos\phi + h))}. \tag{3.2.18}$$

Next, we take the limit $T \to 0$, or $\beta \to \infty$. The one-point function $\langle\sigma^z\rangle$ is reduced to

$$\langle\sigma^z\rangle = \begin{cases} 1 & \text{for } h > J, \\ -1 + \frac{2}{\pi}\arccos(-\frac{h}{J}) & \text{for } h < J; \end{cases} \tag{3.2.19}$$

see Fig. 3.3. Equations (3.2.17) and (3.2.18) behave differently in the two phases $h > J$ and $h < J$:

$$G_{l,l} = \begin{cases} 1 & \text{for } h > J, \\ -1 + \frac{2}{\pi}\arccos(-\frac{h}{J}) & \text{for } h < J, \end{cases} \tag{3.2.20}$$

$$G_{l,m} = \begin{cases} 0 & \text{for } h > J, \\ \frac{2}{\pi}\frac{1}{l-m}\sin[(l-m)\arccos(-\frac{h}{J})] & \text{for } h < J. \end{cases} \tag{3.2.21}$$

We thus have all the necessary correlation functions.

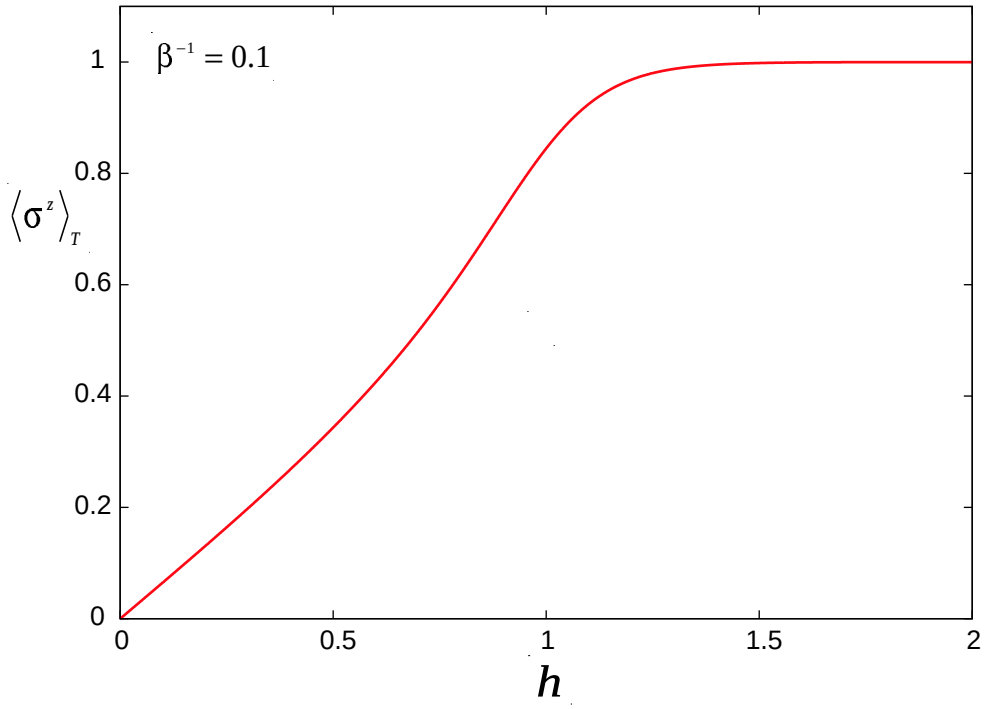

Figure 3.3: The magnetization in the z direction at temperature T as a function of the uniform field for $\beta^{-1} = 0.1$ where the coupling constant J is set to one.

3.2.3 Numerical solution of the XY model in a random magnetic field

Now we consider the case of a random magnetic field at zero temperature $T = 0$, which is the main theme of this thesis. We only outline the procedure. See also Appendix C for details.

The Hamiltonian is given by Eq. (3.1.7), or

$$H = -\frac{J}{2}\sum_{j=1}^{N}(a_j^\dagger a_{j+1} + a_{j+1}^\dagger a_j) - \sum_{j=1}^{N}(h + h_j)\left(a_j^\dagger a_j - \frac{1}{2}\right), \tag{3.2.22}$$

where $\{h_i\}$ are random magnetic fields obeying the probability distribution (3.1.3). The boundary conditions are given by Eq. (3.1.8). Since there is no interaction between the fermions, the problem is reduced to a one-particle problem.

The Hamiltonian (3.2.22) without the constant term is expressed in the form

$$H' = \sum_{j,k} a_j^\dagger A_{j,k} a_k = \boldsymbol{a}^\dagger A \boldsymbol{a} \tag{3.2.23}$$

with

$$A = \begin{pmatrix} -h-h_1 & -\frac{J}{2} & 0 & \cdots & 0 & \pm\frac{J}{2} \\ -\frac{J}{2} & -h-h_2 & -\frac{J}{2} & 0 & \vdots & 0 \\ 0 & -\frac{J}{2} & \ddots & \ddots & 0 & \vdots \\ \vdots & 0 & \ddots & \ddots & -\frac{J}{2} & 0 \\ 0 & \vdots & \ddots & -\frac{J}{2} & -h-h_{N-1} & -\frac{J}{2} \\ \pm\frac{J}{2} & 0 & \cdots & 0 & -\frac{J}{2} & -h-h_N \end{pmatrix}, \tag{3.2.24}$$

where the signs of the $(1, N)$ and $(N, 1)$ elements depend on the boundary conditions (3.1.8); the sign is negative for even N_F and positive for odd N_F. The vectors $\boldsymbol{a}$ and $\boldsymbol{a}^\dagger$ denote

$$\boldsymbol{a} = \begin{pmatrix} a_1 \\ a_2 \\ \vdots \\ a_{N-1} \\ a_N \end{pmatrix}, \quad \boldsymbol{a}^\dagger = \begin{pmatrix} a_1^\dagger & a_2^\dagger & \cdots & a_{N-1}^\dagger & a_N^\dagger \end{pmatrix}. \tag{3.2.25}$$

As Eq. (3.2.24) is Hermitian, there exists a unitary matrix V such that $V^\dagger A V = \Lambda$ is a diagonal matrix. We thus have

$$H' = \boldsymbol{a}^\dagger A \boldsymbol{a} = \boldsymbol{c}^\dagger \Lambda \boldsymbol{c} \tag{3.2.26}$$

with

$$\begin{aligned} c_m^\dagger &= \sum_j a_j^\dagger V_{jm}, \\ c_m &= \sum_j V_{mj}^\dagger a_j, \end{aligned} \tag{3.2.27}$$

where $c_m^\dagger$ and c_m satisfy the anti-commutation relations $\{c_n^\dagger, c_m\} = \delta_{nm}$ and $\{c_n, c_m\} = 0$. We here write the inverse transformation of Eq. (3.2.27) as

$$\begin{aligned} a_j^\dagger &= \sum_m c_m^\dagger V_{mj}^\dagger, \\ a_j &= \sum_m V_{jm} c_m. \end{aligned} \tag{3.2.28}$$

Once we diagonalize the matrix (3.2.24), we can construct the ground state of the many-body Hamiltonian (3.2.22). Let $\epsilon_1, \epsilon_2, \cdots \epsilon_{N_G}, \epsilon_{N_G+1}, \cdots \epsilon_{N-1}, \epsilon_N$ denote the eigenvalues of the matrix (3.2.24) in the ascending order. If $\epsilon_{N_G} < 0$ and $\epsilon_{N_G+1} > 0$, the ground state of the Hamiltonian (3.2.22) is given by

$$|\mathrm{Gs}\rangle = c_{N_G}^\dagger c_{N_G-1}^\dagger \cdots c_2^\dagger c_1^\dagger |0\rangle. \tag{3.2.29}$$

Now we are in the position of calculating the one-point and two-point correlation functions. We here merely summarize the results:

$$\langle \sigma_i^z \rangle = G_{i,i}, \tag{3.2.30}$$

$$\langle \sigma_i^x \sigma_j^x \rangle = \begin{vmatrix} G_{i,i+1} & G_{i,i+2} & \cdots & G_{i,j} \\ G_{i+1,i+1} & G_{i+1,i+2} & \cdots & G_{i+1,j} \\ \vdots & \vdots & \ddots & \vdots \\ G_{j-1,i+1} & G_{j-1,i+2} & \cdots & G_{j-1,j} \end{vmatrix}, \tag{3.2.31}$$

$$\langle \sigma_i^y \sigma_j^y \rangle = \begin{vmatrix} G_{i+1,i} & G_{i+2,i} & \cdots & G_{j,i} \\ G_{i+1,i+1} & G_{i+2,i+1} & \cdots & G_{j,i+1} \\ \vdots & \vdots & \ddots & \vdots \\ G_{i+1,j-1} & G_{i+2,j-1} & \cdots & G_{j,j-1} \end{vmatrix}, \tag{3.2.32}$$

$$\langle \sigma_i^z \sigma_j^z \rangle = \begin{vmatrix} G_{i,i} & G_{i,j} \\ G_{j,i} & G_{j,j} \end{vmatrix}, \tag{3.2.33}$$

with

$$G_{i,j} = 2 \sum_{m=1}^{N_G} V_{im} V_{jm} - \delta_{ij}. \tag{3.2.34}$$

The magnetization in the z direction (3.2.30) is plotted as a function of the uniform field in Fig. 3.4. The singularity of the derivative of the magnetization vanishes. The reduction of the magnetization for $q = 2$ is greater than that of the magnetization for $q = 1$.

In the case $q = 2$, Nishimori [28] analytically calculated one-point functions and obtained lower bounds of the two-point functions. The results in the paper [28], however, are not used in the present thesis, since we take the random average of the concurrence, a non-linear function of the one-point and two-point functions, as we show in the next few sections.

3.3 The concurrence

3.3.1 Formula for the isotropic XY model

We now measure the entanglement between the spins using the concurrence (2.2.11). We first remind readers of how to calculate the concurrence. The concurrence of the spins between the sites i and j is given by

$$C(\rho_{ij}) = \max\{0, \lambda_1 - \lambda_2 - \lambda_3 - \lambda_4\}, \tag{3.3.1}$$

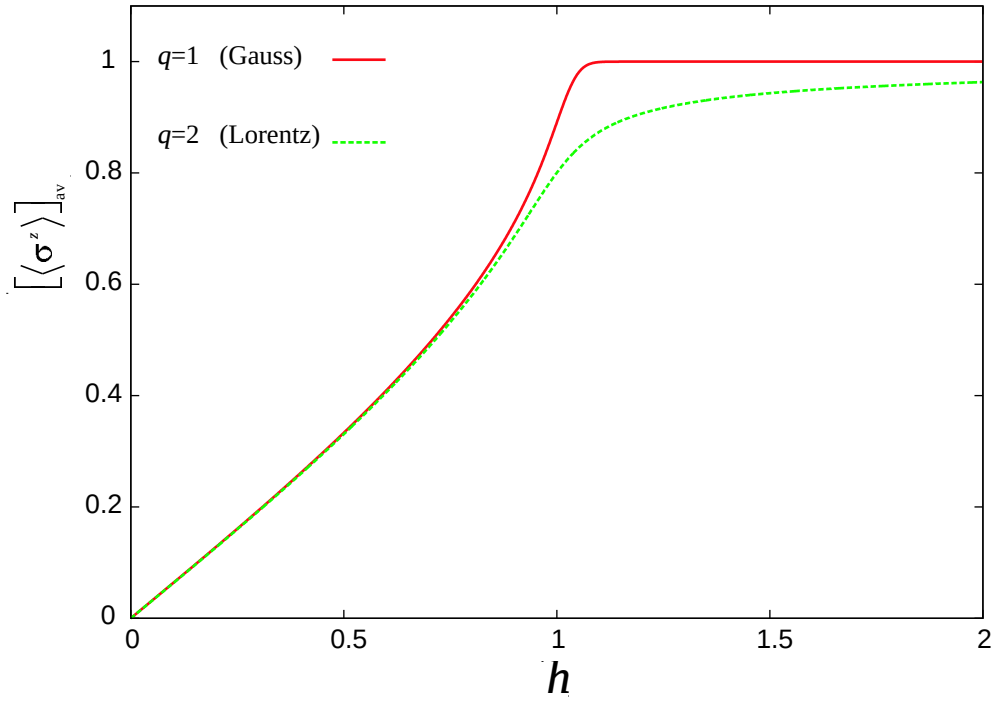

Figure 3.4: The average magnetization $[\langle\sigma^z\rangle]_{\rm av}$ in the z direction at zero temperature $T = 0$ in a random magnetic field as a function of the uniform field, where $[\cdots]_{\rm av}$ denotes the random average. The red line indicates the case $q = 1$ (a Gaussian distribution) with $a = 0.1$ and the green line indicates the case $q = 2$ (a Lorentzian distribution) with $a = 0.1$.

where $\{\lambda_i\}$ are the square roots of the eigenvalues of the matrix $R_{ij} = \rho_{ij}\tilde{\rho}_{ij}$ in the descending order, $\lambda_1 \geq \lambda_2 \geq \lambda_3 \geq \lambda_4$, with $\tilde{\rho}_{ij} = (\sigma_i^y \otimes \sigma_j^y)\rho_{ij}^*(\sigma_i^y \otimes \sigma_j^y)$, and ρ_{ij} is the 4×4 reduced density matrix given by

$$\rho_{ij} = {\rm Tr}_{\hat{ij}}\rho \tag{3.3.2}$$

with ${\rm Tr}_{\hat{ij}}$ denoting the trace over the degrees of freedom except for the sites i and j (see Eq. (1.2.16)).

Thus we first calculate the square roots of the eigenvalues of the matrix $R_{ij} = \rho_{ij}\tilde{\rho}_{ij}$. We write down the 4×4 matrix R_{ij} as

$$\begin{aligned} R_{ij} = \frac{1}{16}\Bigg(I_{ij} + \langle\sigma_i^z\rangle\sigma_i^z \otimes I_j + \langle\sigma_j^z\rangle I_i \otimes \sigma_j^z + \sum_{\alpha=x,y,z}\langle\sigma_i^\alpha\sigma_j^\alpha\rangle\sigma_i^\alpha \otimes \sigma_j^\alpha\Bigg) \\ \times\Bigg(I_{ij} - \langle\sigma_i^z\rangle\sigma_i^z \otimes I_j - \langle\sigma_j^z\rangle I_i \otimes \sigma_j^z + \sum_{\alpha=x,y,z}\langle\sigma_i^\alpha\sigma_j^\alpha\rangle\sigma_i^\alpha \otimes \sigma_j^\alpha\Bigg), \end{aligned} \tag{3.3.3}$$

where we note $\langle\sigma_i^x\sigma_j^x\rangle = \langle\sigma_i^y\sigma_j^y\rangle$. We then introduce the 4×4 matrices T and S:

$$T = \begin{pmatrix} 0 & 1 & 0 & 0 \\ 0 & 0 & 1 & 0 \\ 1 & 0 & 0 & 0 \\ 0 & 0 & 0 & 1 \end{pmatrix}, \quad S = \begin{pmatrix} 1 & 0 & 0 & 0 \\ 0 & \frac{1}{\sqrt{2}} & \frac{1}{\sqrt{2}} & 0 \\ 0 & -\frac{1}{\sqrt{2}} & \frac{1}{\sqrt{2}} & 0 \\ 0 & 0 & 0 & 1 \end{pmatrix}. \tag{3.3.4}$$

The matrices T and S block-diagonalize the matrix R_{ij} as

$$(TS)R(TS)^{-1} = \frac{1}{16}\begin{pmatrix} a^- & b^+ & 0 & 0 \\ b^- & a^+ & 0 & 0 \\ 0 & 0 & c & 0 \\ 0 & 0 & 0 & c \end{pmatrix}, \tag{3.3.5}$$

where a^+, a^-, b^+, b^- and c are given by

$$a^\pm = 4\langle\sigma_i^x\sigma_j^x\rangle^2 \pm 4\langle\sigma_i^x\sigma_j^x\rangle\left(-1+\langle\sigma_i^z\sigma_j^z\rangle\right) + \left(\langle\sigma_i^z\sigma_j^z\rangle - 1\right)^2 - \left(\langle\sigma_i^z\rangle - \langle\sigma_i^z\rangle\right)^2, \tag{3.3.6}$$

$$b^\pm = \pm 4\langle\sigma_i^x\sigma_j^x\rangle^2\left(\langle\sigma_i^z\rangle - \langle\sigma_i^z\rangle\right), \tag{3.3.7}$$

and

$$c \;= \left(1+\langle\sigma_i^x\sigma_j^x\rangle - \langle\sigma_i^z\rangle - \langle\sigma_j^z\rangle\right)\left(1+\langle\sigma_i^x\sigma_j^x\rangle + \langle\sigma_i^z\rangle + \langle\sigma_j^z\rangle\right). \tag{3.3.8}$$

Thus the characteristic equation can be reduced to be quadratic. After some algebra, we arrive at the square roots of the eigenvalues of the matrix R_{ij} in the forms

$$\frac{1}{4}\sqrt{\left(1+\langle\sigma_i^x\sigma_j^x\rangle - \langle\sigma_i^z\rangle - \langle\sigma_j^z\rangle\right)\left(1+\langle\sigma_i^x\sigma_j^x\rangle + \langle\sigma_i^z\rangle + \langle\sigma_j^z\rangle\right)}, \tag{3.3.9}$$

and

$$\frac{1}{4}\sqrt{4\langle\sigma_i^x\sigma_j^x\rangle + (\langle\sigma_i^z\sigma_j^z\rangle - 1)^2 - (\langle\sigma_i^z\rangle + \langle\sigma_j^z\rangle)^2 \pm 4\sqrt{\langle\sigma_i^x\sigma_j^x\rangle^2\left[(\langle\sigma_i^z\sigma_j^z\rangle - 1)^2 - (\langle\sigma_i^z\rangle + \langle\sigma_j^z\rangle)^2\right]}}, \tag{3.3.10}$$

where the eigenvalue (3.3.9) is two-fold degenerate.

3.3.2 The concurrence of the XY model in a uniform field at T

First, we study the entanglement between two spins in a uniform field at zero temperature so that we can compare it to the concurrence in a random magnetic field.

We immediately obtain the concurrence by using Eqs. (3.2.14)–(3.2.16), (3.2.19)–(3.2.21), (3.3.1), (3.3.9) and (3.3.10). Figure 3.5 shows the nearest-neighbor concurrence $C(1)$, the next-nearest-neighbor concurrence $C(2)$, the third-neighbor concurrence $C(3)$, the fourth-neighbor concurrence $C(4)$, and the fifth-neighbor concurrence $C(5)$. We note that the concurrences of the model depend only on the distance $r = |i-j|$, because the model in a

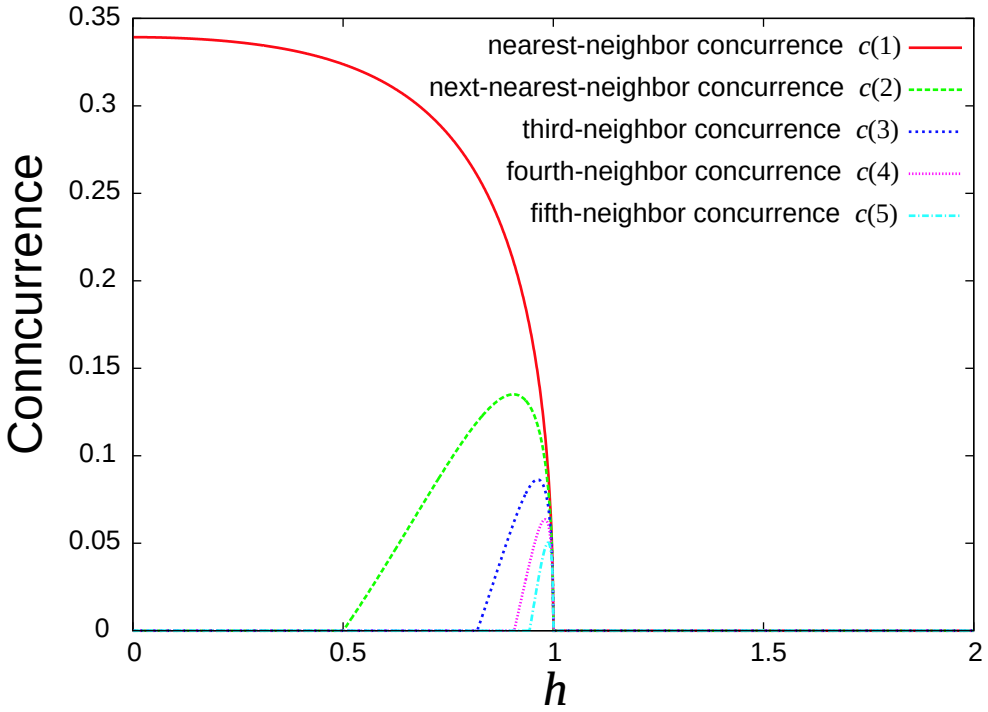

Figure 3.5: The concurrence of the XY model in a uniform field.

uniform field (3.2.10) possesses the translational invariance. The one-point and two-point correlation functions are functions of the distance r; see §3.2.2.

The concurrences rapidly decrease near $h = 1$ and vanish in the region $h > 1$. In the region $h > 1$, the ground state is given by the tensor product of the one-spin state as $|\uparrow\rangle$

$$|\uparrow_1\rangle|\uparrow_2\rangle|\uparrow_3\rangle\cdots, \tag{3.3.11}$$

where $|\uparrow\rangle$ denotes the eigenstate of the operator σ^z satisfying the eigenequation $\sigma^z|\uparrow\rangle = |\uparrow\rangle$. Thus there is no entanglement.

3.3.3 The entanglement of the XY model in a random magnetic field

We here numerically study the entanglement of the XY model in a random magnetic field at zero temperature which is the main theme of the present thesis. The model that we consider is given by Eq. (3.1.1). The probability distribution of the random magnetic field h_j is given by Eq. (3.1.3). We here study the cases $q = 1$ (a Gaussian distribution), $q = 1.35$, $q = 5/3$, $q = 1.85$ and $q = 2$ (a Lorentzian distribution). To generate the random numbers, we used the transformation method for $q = 1$ and for $q = 2$, and used the rejection method for $q = 1.35$, $q = 5/3$ and $q = 1.85$.

We take the random average and the spatial average to evaluate the concurrence. We define the average concurrence as

$$C(r) = \frac{1}{N}\sum_{i=1}^{N}\left[C_{i,i+r}\right]_{\rm av}, \tag{3.3.12}$$

where $[\cdots]_{\rm av}$ denotes the random average, $C_{i,j}$ denotes the concurrence between the sites i and j, and N is the number of the sites.

The random average of the entanglement of formation is always greater than that obtained by substitution of the random average of concurrence into Eq. (2.2.9). This is shown by the fact that $E(\rho)$ in Eq. (2.2.9) is a concave function of the concurrence as seen in Fig. 2.2. Any concave function $f(x)$ with a real number x satisfies the relation

$$\sum_i p_i f(x_i) \geq f\left(\sum_i p_i x_i\right), \tag{3.3.13}$$

where p_i (> 0) satisfies $\sum_i p_i = 1$. We thus have

$$\left[E(C)\right]_{\rm av} \geq E\left(\left[C\right]_{\rm av}\right), \tag{3.3.14}$$

where

$$E(C) = -\frac{1+\sqrt{1-C^2}}{2}\log_2\left(\frac{1+\sqrt{1-C^2}}{2}\right) - \frac{1-\sqrt{1-C^2}}{2}\log_2\left(\frac{1-\sqrt{1-C^2}}{2}\right); \tag{3.3.15}$$

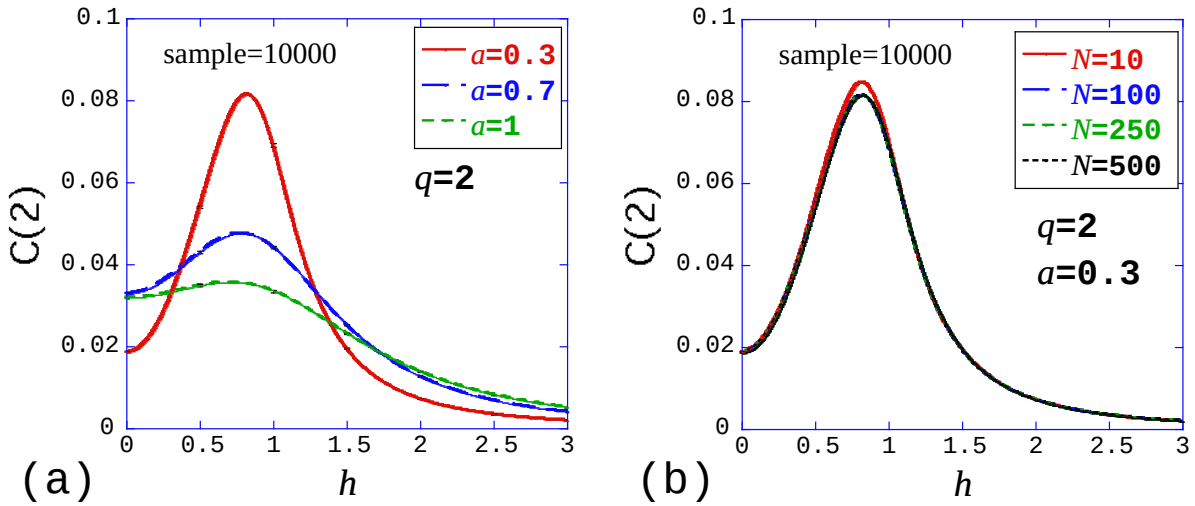

Figure 3.6: (a) The next-nearest-neighbor concurrences for $q = 2$ (Lorentz) with the scale parameter $a = 0.3$, 0.7, 1. All the lines are plotted as a function of the uniform field h and are taken the random average 10000 times. (b) The next-nearest-neighbor concurrences for $q = 2$ (Lorentz). The lines are plotted with the scale parameter $a = 0.3$ and for the system size $N = 10$, 100, 250, 500.

see Eqs. (2.2.9) and (2.2.10). Therefore, if the random average of the concurrence does not vanish, the random average of the entanglement of formation does not vanish either.

We evaluated the concurrences numerically by using Eqs. (3.2.30)–(3.2.34), (3.3.9), (3.3.10) and (3.3.1), having Figs. 3.8–3.12. For all the results, the number of the sites N is 500 and the number of the samples is 10000. In Fig. 3.6(a), the next-nearest-neighbor concurrences are plotted for $q = 2$ with error bars at $h = 0$, 0.5, 1, 1.5, 2, 2.5 and 3, but the errors are negligible. In Fig. 3.6(b), the next-nearest-neighbor concurrence is plotted for $q = 2$ and for the system size $N = 10$, 100, 250 and 500 with the random average over 10000 samples. The finite-size effect is invisible for $N \geq 100$. Hence, we conclude that 10000 samples and the system size $N = 500$ are substantial.

The nearest-neighbor concurrence for all cases in Fig. 3.8 behaves similarly. In the region $h < 1$, the nearest-neighbor concurrence in the random magnetic field for each q decreases as the distribution width a is increased. The reduction of the nearest-neighbor concurrence is greater as the scale parameter a is increased. In the region $h > 1$, the nearest-neighbor concurrence for all q is restored by the random magnetic field. That is, the random magnetic field restores the quantum correlation. We use the term "restore" in the following sense: Though the quantum XY spin chain is reduced to the classical Ising model by increasing the uniform field ($h > 1$), the model restores the quantum property after introducing the random magnetic field in the region of $h > 1$. The reason why the nearest-neighbor concurrence is restored in the $h > 1$ may be as follows; the random

magnetic field flips some spins and flipped spins and their neighboring spins restore the quantum interaction.

As shown in Fig. 3.9, the next-nearest neighbor concurrence for each q is decreased in the region $0.5 < h < 1$ as the scale parameter a is increased. On the other hand, in the regions $h < 1/2$ and $h > 1$ it is restored as the randomness a is increased. There may be some situations that restores the next-nearest-neighbor concurrence in $h < 1/2$. If the random magnetic field is almost constant as, say, $h_i \approx 0.7$ over a region with $h = 0$, the next-nearest-neighbor concurrence can be finite; see Fig. 3.7(a). Another possibility is following. Suppose that a strong magnetic field happens to occur at a site as in Fig. 3.7(b). We can take the Zeeman energy of the site exposed to the strong magnetic field as the non-perturbation term and calculate the second-order perturbation of the exchange energy. We may end up with an effective interaction between the two neighboring spins of the spin exposed to the strong magnetic field. In this situation, the next-nearest-neighbor concurrence may be restored. We, however, have not been able to determine the reason of the restoration in $h < 1/2$ decidedly.

We find that the qualitative behavior of the next-nearest neighbor concurrence is different depending on whether the variance of the distribution function is finite or not. The maximum point of the next-nearest-neighbor concurrence for the cases $q < 5/3$, where the variance of the distribution function is finite, shifts to the right as the randomness a is increased as shown in Fig. 3.9(a) and Fig. 3.9(b). In contrast, the maximum point of the next-nearest-neighbor concurrence for the cases $q \geq 5/3$ in Fig. 3.9(c)–(e) shifts to the left as the randomness a is increased. The third-neighbor concurrence and the rest behave similarly to the next-nearest-neighbor concurrence, but have a little differences from the next-nearest-neighbor concurrences. The third-neighbor concurrences and the rest are smaller than the nearest-neighbor concurrences. The maximum point of the third neighbor concurrences and the rest for the cases $q \leq 5/3$ first shift to the left and turn to the right as shown in Figs. 3.10–3.12.

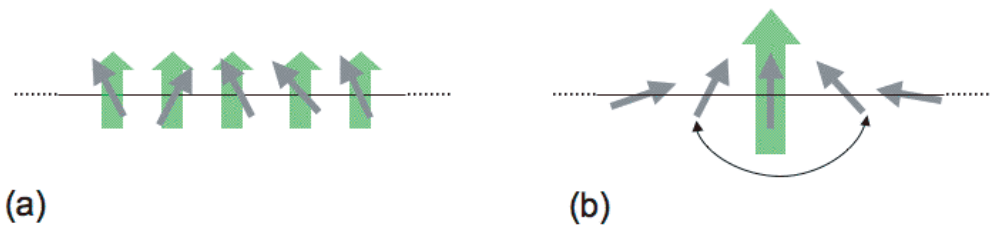

Figure 3.7: Block arrows indicate spins. Green arrows indicate random magnetic field

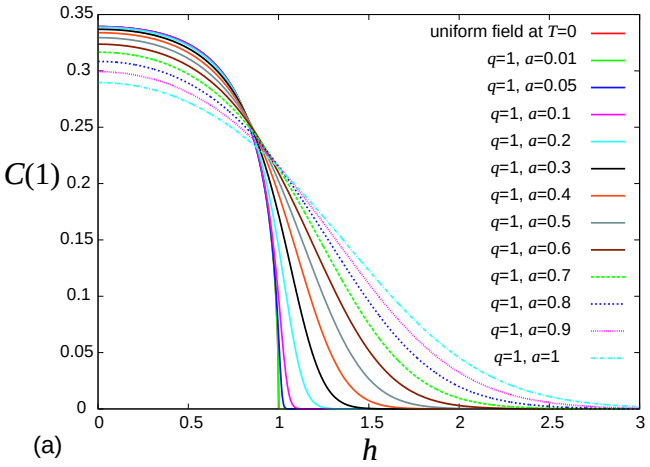
0.35
0.3
0.25
0.2
0.15
0.1
0.05
0
C(1)
0
0.5
1
1.5
2
2.5
3
h
uniform field at T=0
q=1, a=0.01
q=1, a=0.05
q=1, a=0.1
q=1, a=0.2
q=1, a=0.3
q=1, a=0.4
q=1, a=0.5
q=1, a=0.6
q=1, a=0.7
q=1, a=0.8
q=1, a=0.9
q=1, a=1

(a)

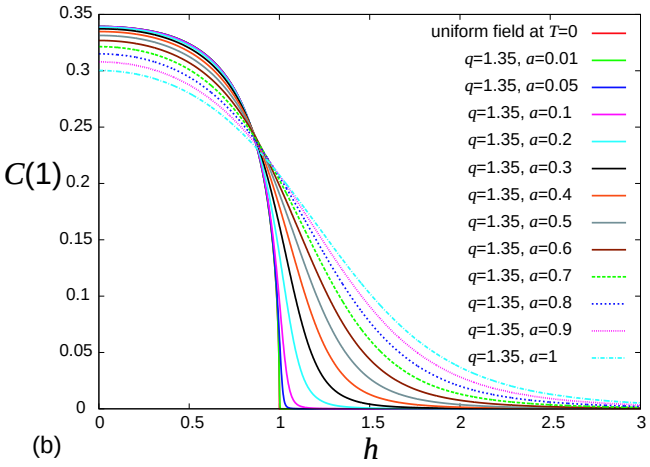
0.35
0.3
0.25
0.2
0.15
0.1
0.05
0
C(1)
0
0.5
1
1.5
2
2.5
3
h
uniform field at T=0
q=1.35, a=0.01
q=1.35, a=0.05
q=1.35, a=0.1
q=1.35, a=0.2
q=1.35, a=0.3
q=1.35, a=0.4
q=1.35, a=0.5
q=1.35, a=0.6
q=1.35, a=0.7
q=1.35, a=0.8
q=1.35, a=0.9
q=1.35, a=1

(b)

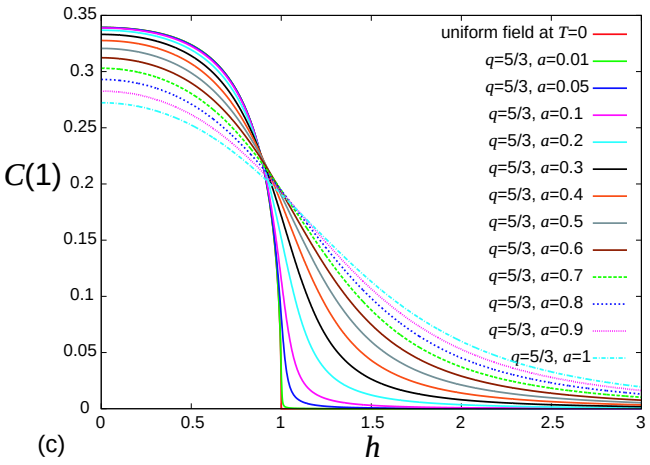
0.35
0.3
0.25
0.2
0.15
0.1
0.05
0
C(1)
0
0.5
1
1.5
2
2.5
3
h
uniform field at T=0
q=5/3, a=0.01
q=5/3, a=0.05
q=5/3, a=0.1
q=5/3, a=0.2
q=5/3, a=0.3
q=5/3, a=0.4
q=5/3, a=0.5
q=5/3, a=0.6
q=5/3, a=0.7
q=5/3, a=0.8
q=5/3, a=0.9
q=5/3, a=1

(c)

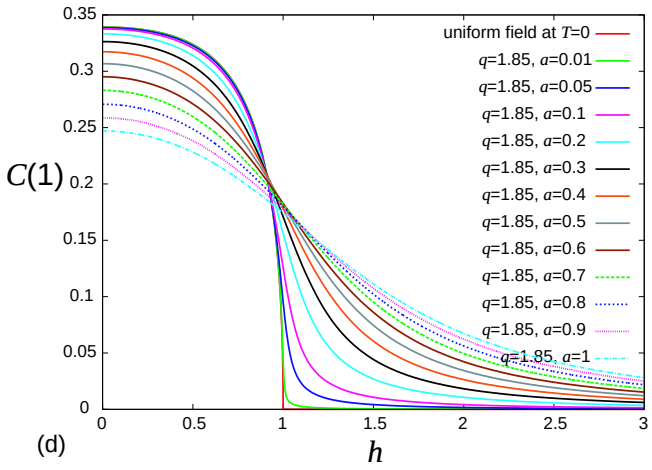

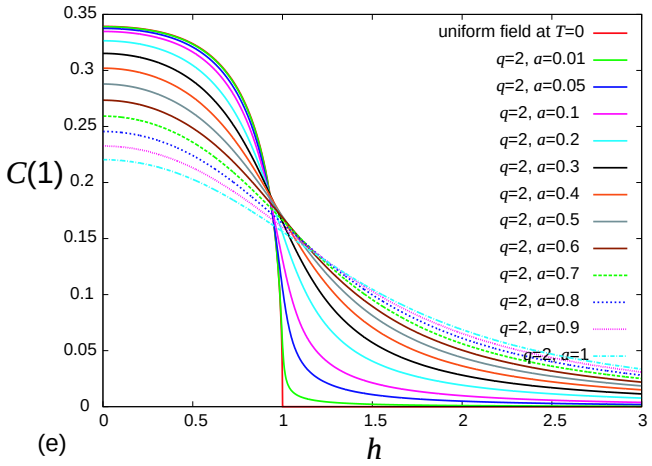

Figure 3.8: (a) The nearest-neighbor concurrence for $q = 1$ (Gauss); (b) The nearest-neighbor concurrence for $q = 1.35$; (c) The nearest-neighbor concurrence for $q = 5/3$; (d) The nearest-neighbor concurrence for $q = 1.85$; (e) The nearest-neighbor concurrence for $q = 2$ (Lorentz). All the data are plotted as functions of the uniform field for $N = 500$.

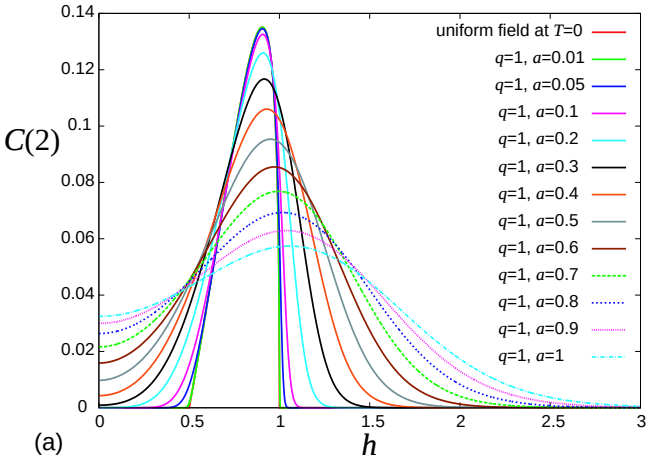
C(2)
h
uniform field at T=0
q=1, a=0.01
q=1, a=0.05
q=1, a=0.1
q=1, a=0.2
q=1, a=0.3
q=1, a=0.4
q=1, a=0.5
q=1, a=0.6
q=1, a=0.7
q=1, a=0.8
q=1, a=0.9
q=1, a=1

(a)

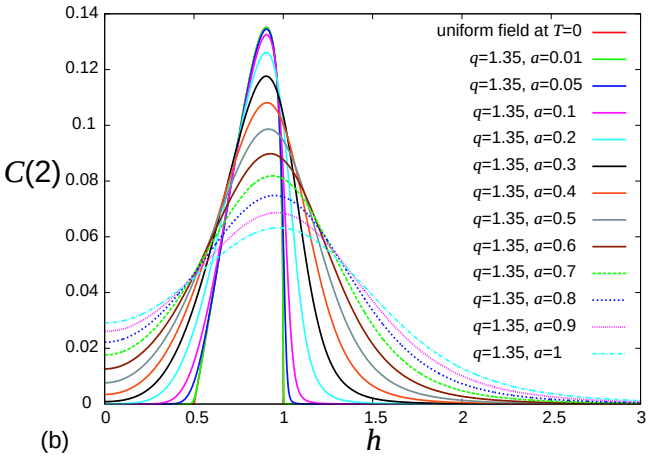
C(2)
h
uniform field at T=0
q=1.35, a=0.01
q=1.35, a=0.05
q=1.35, a=0.1
q=1.35, a=0.2
q=1.35, a=0.3
q=1.35, a=0.4
q=1.35, a=0.5
q=1.35, a=0.6
q=1.35, a=0.7
q=1.35, a=0.8
q=1.35, a=0.9
q=1.35, a=1

(b)

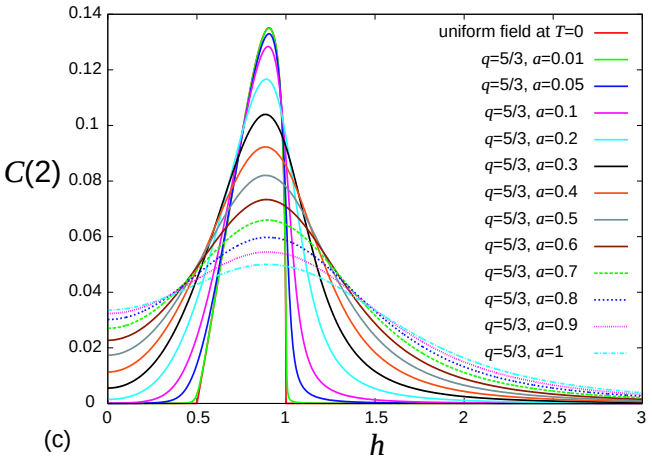
C(2)
h
uniform field at T=0
q=5/3, a=0.01
q=5/3, a=0.05
q=5/3, a=0.1
q=5/3, a=0.2
q=5/3, a=0.3
q=5/3, a=0.4
q=5/3, a=0.5
q=5/3, a=0.6
q=5/3, a=0.7
q=5/3, a=0.8
q=5/3, a=0.9
q=5/3, a=1

(c)

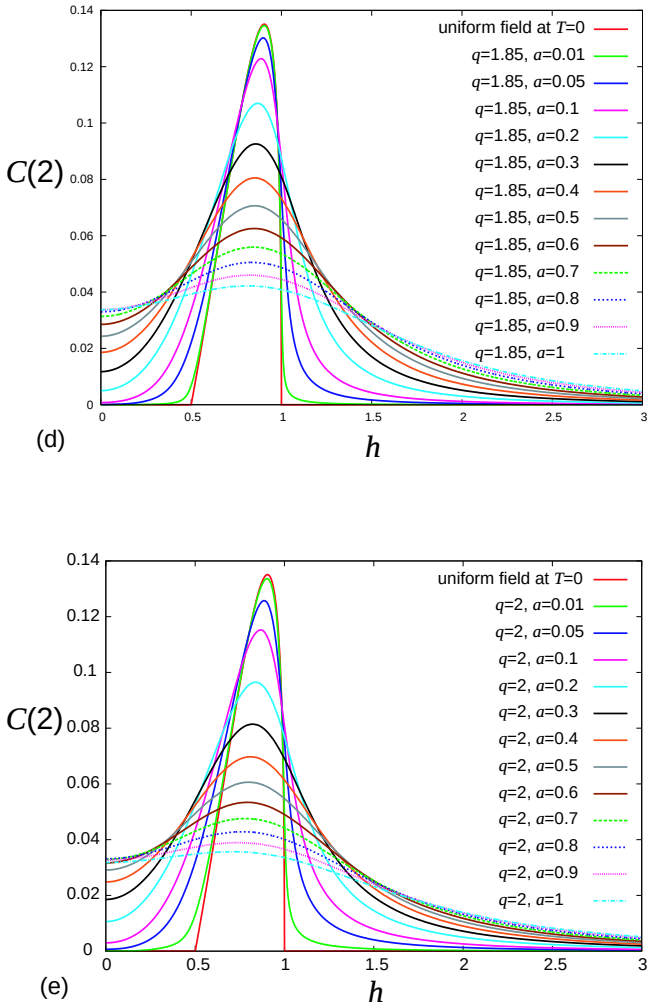

Figure 3.9: (a) The next-neighbor concurrence for $q = 1$ (Gauss); (b) The next-neighbor concurrence for $q = 1.35$; (c) The next-neighbor concurrence for $q = 5/3$; (d) The next-neighbor concurrence for $q = 1.85$; (e) The next-neighbor concurrence for $q = 2$ (Lorentz). All the data are plotted as functions of the uniform field for $N = 500$.

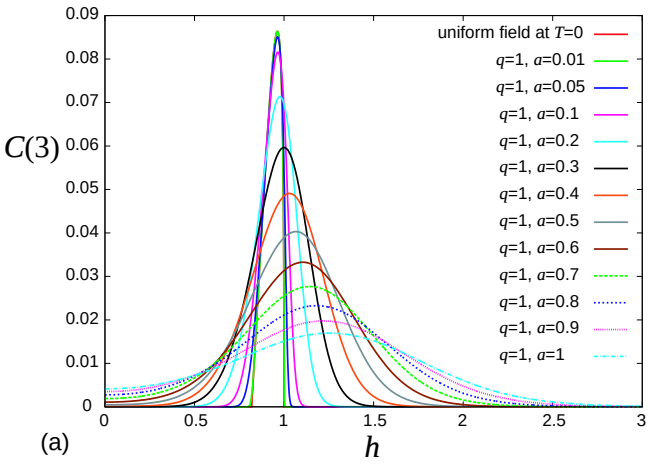
C(3)
h
uniform field at T=0
q=1, a=0.01
q=1, a=0.05
q=1, a=0.1
q=1, a=0.2
q=1, a=0.3
q=1, a=0.4
q=1, a=0.5
q=1, a=0.6
q=1, a=0.7
q=1, a=0.8
q=1, a=0.9
q=1, a=1

(a)

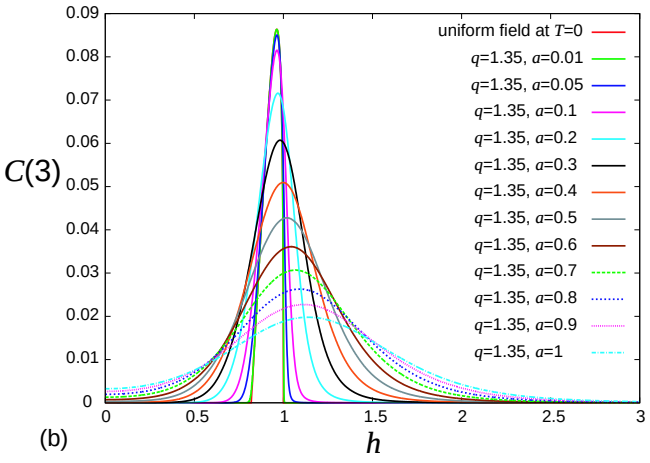
C(3)
h
uniform field at T=0
q=1.35, a=0.01
q=1.35, a=0.05
q=1.35, a=0.1
q=1.35, a=0.2
q=1.35, a=0.3
q=1.35, a=0.4
q=1.35, a=0.5
q=1.35, a=0.6
q=1.35, a=0.7
q=1.35, a=0.8
q=1.35, a=0.9
q=1.35, a=1

(b)

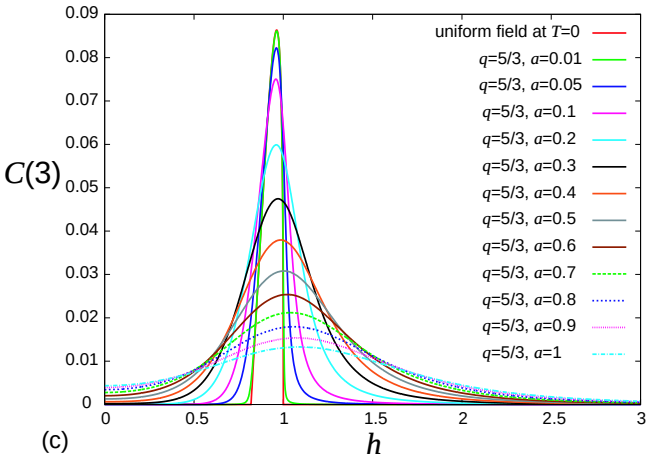
C(3)
h
uniform field at T=0
q=5/3, a=0.01
q=5/3, a=0.05
q=5/3, a=0.1
q=5/3, a=0.2
q=5/3, a=0.3
q=5/3, a=0.4
q=5/3, a=0.5
q=5/3, a=0.6
q=5/3, a=0.7
q=5/3, a=0.8
q=5/3, a=0.9
q=5/3, a=1

(c)

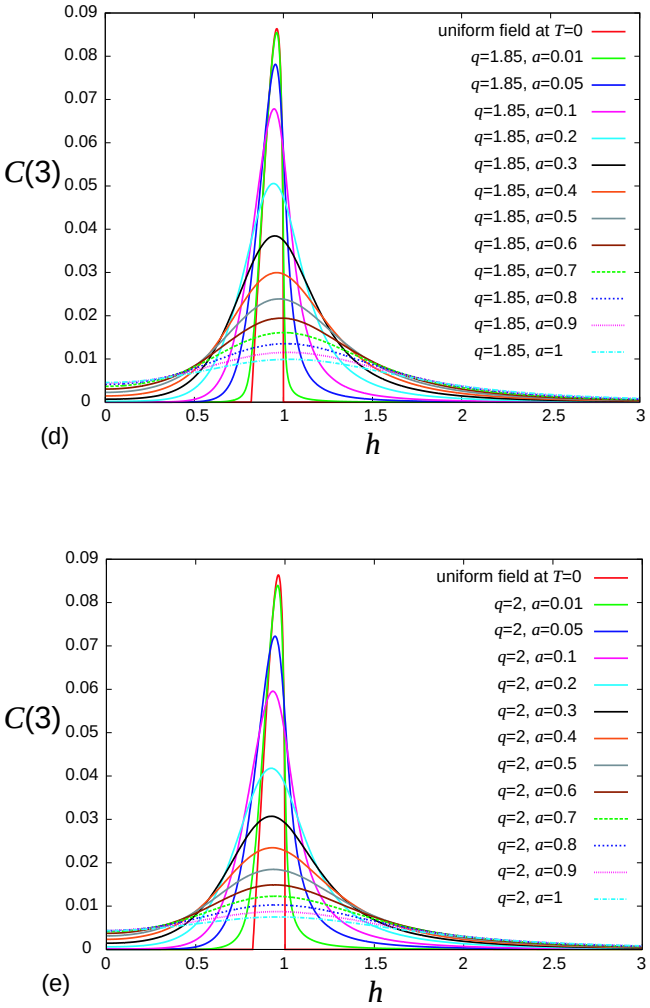

Figure 3.10: (a) The third neighbor concurrence for $q = 1$ (Gauss); (b) The third neighbor concurrence for $q = 1.35$; (c) The third neighbor concurrence for $q = 5/3$; (d) The third neighbor concurrence for $q = 1.85$; (e) The third neighbor concurrence for $q = 2$ (Lorentz). All the data are plotted as functions of the uniform field for $N = 500$.

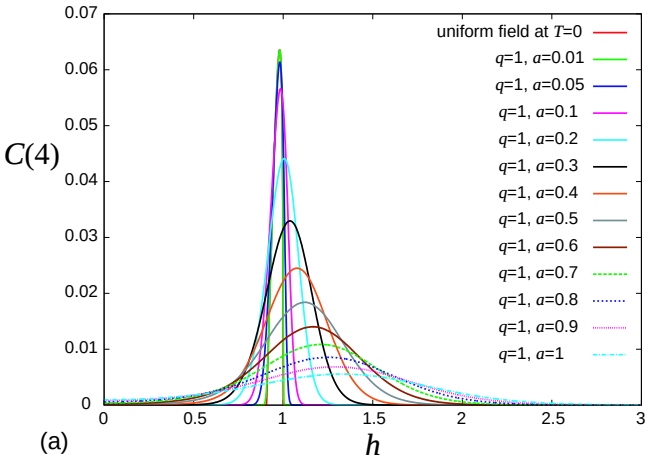
C(4)
h
uniform field at T=0
q=1, a=0.01
q=1, a=0.05
q=1, a=0.1
q=1, a=0.2
q=1, a=0.3
q=1, a=0.4
q=1, a=0.5
q=1, a=0.6
q=1, a=0.7
q=1, a=0.8
q=1, a=0.9
q=1, a=1

(a)

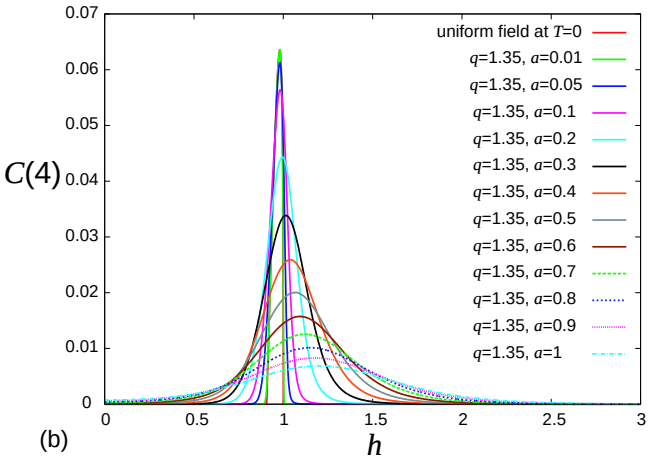
C(4)
h
uniform field at T=0
q=1.35, a=0.01
q=1.35, a=0.05
q=1.35, a=0.1
q=1.35, a=0.2
q=1.35, a=0.3
q=1.35, a=0.4
q=1.35, a=0.5
q=1.35, a=0.6
q=1.35, a=0.7
q=1.35, a=0.8
q=1.35, a=0.9
q=1.35, a=1

(b)

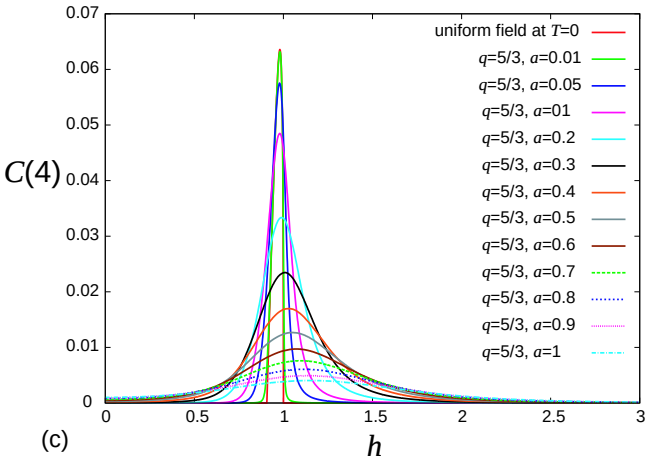
C(4)
h
uniform field at T=0
q=5/3, a=0.01
q=5/3, a=0.05
q=5/3, a=01
q=5/3, a=0.2
q=5/3, a=0.3
q=5/3, a=0.4
q=5/3, a=0.5
q=5/3, a=0.6
q=5/3, a=0.7
q=5/3, a=0.8
q=5/3, a=0.9
q=5/3, a=1

(c)

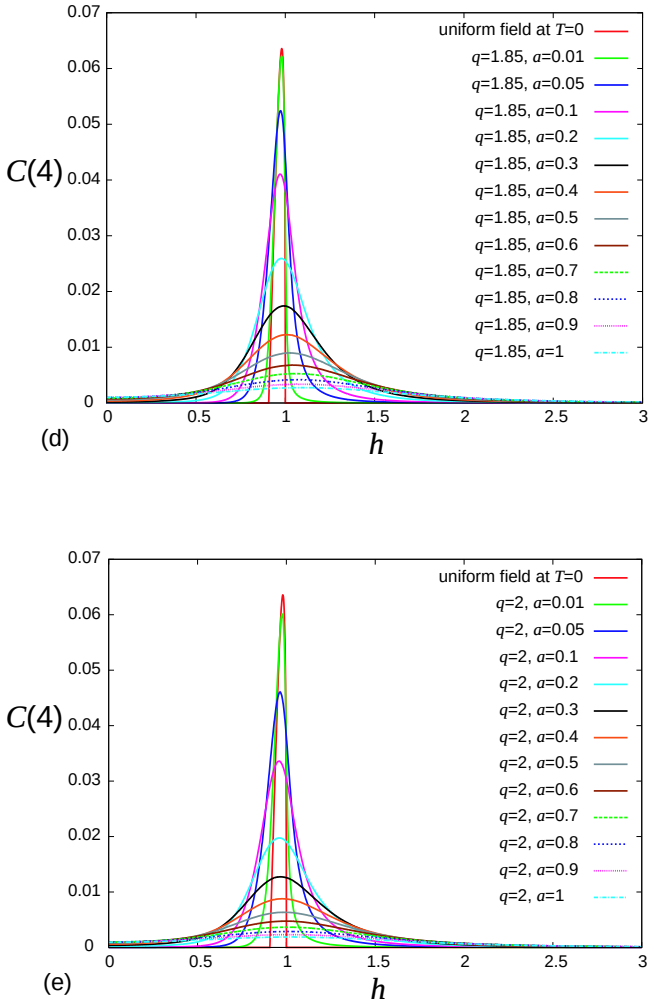

Figure 3.11: (a) The fourth neighbor concurrence for $q = 1$ (Gauss); (b) The fourth neighbor concurrence for $q = 1.35$; (c) The fourth neighbor concurrence for $q = 5/3$; (d) The fourth neighbor concurrence for $q = 1.85$; (e) The fourth neighbor concurrence for $q = 2$ (Lorentz). All the data are plotted as functions of the uniform field for $N = 500$.

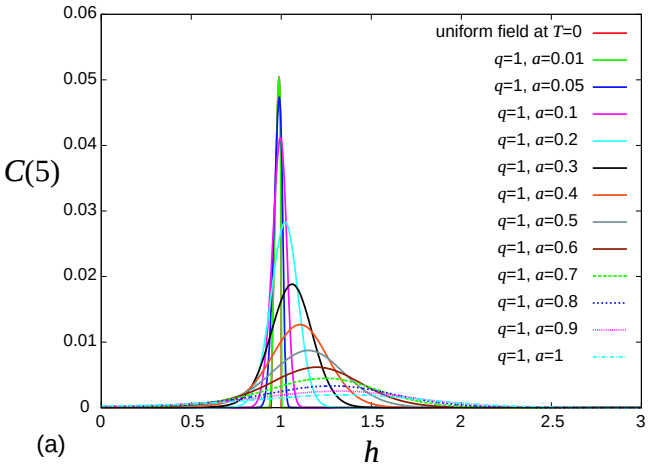
0.06
0.05
0.04
0.03
0.02
0.01
0
C(5)
0
0.5
1
1.5
2
2.5
3
h
uniform field at T=0
q=1, a=0.01
q=1, a=0.05
q=1, a=0.1
q=1, a=0.2
q=1, a=0.3
q=1, a=0.4
q=1, a=0.5
q=1, a=0.6
q=1, a=0.7
q=1, a=0.8
q=1, a=0.9
q=1, a=1

(a)

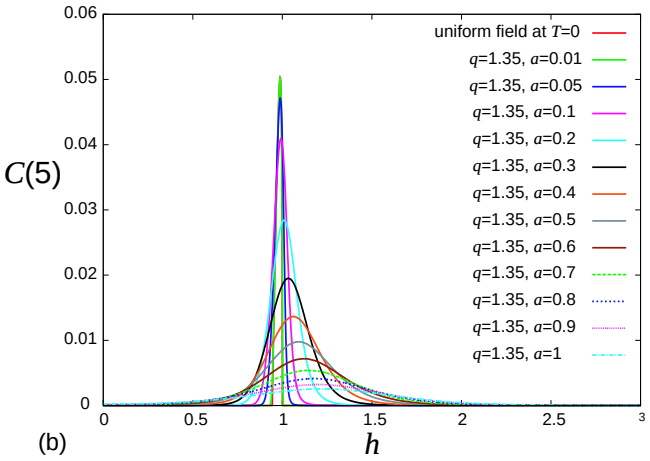
0.06
0.05
0.04
0.03
0.02
0.01
0
C(5)
0
0.5
1
1.5
2
2.5
3
h
uniform field at T=0
q=1.35, a=0.01
q=1.35, a=0.05
q=1.35, a=0.1
q=1.35, a=0.2
q=1.35, a=0.3
q=1.35, a=0.4
q=1.35, a=0.5
q=1.35, a=0.6
q=1.35, a=0.7
q=1.35, a=0.8
q=1.35, a=0.9
q=1.35, a=1

(b)

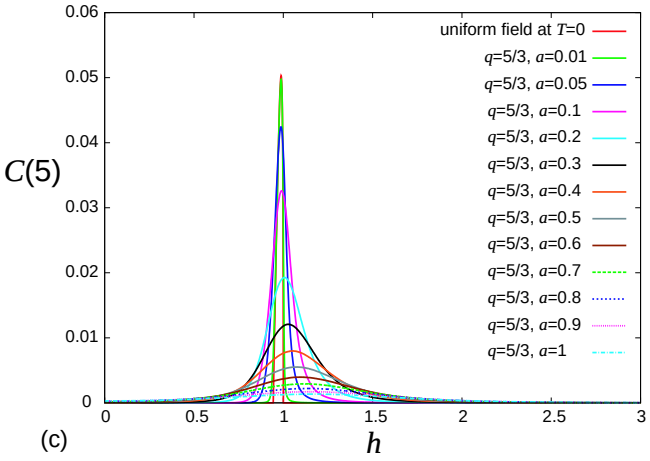
0.06
0.05
0.04
0.03
0.02
0.01
0
C(5)
0
0.5
1
1.5
2
2.5
3
h
uniform field at T=0
q=5/3, a=0.01
q=5/3, a=0.05
q=5/3, a=0.1
q=5/3, a=0.2
q=5/3, a=0.3
q=5/3, a=0.4
q=5/3, a=0.5
q=5/3, a=0.6
q=5/3, a=0.7
q=5/3, a=0.8
q=5/3, a=0.9
q=5/3, a=1

(c)

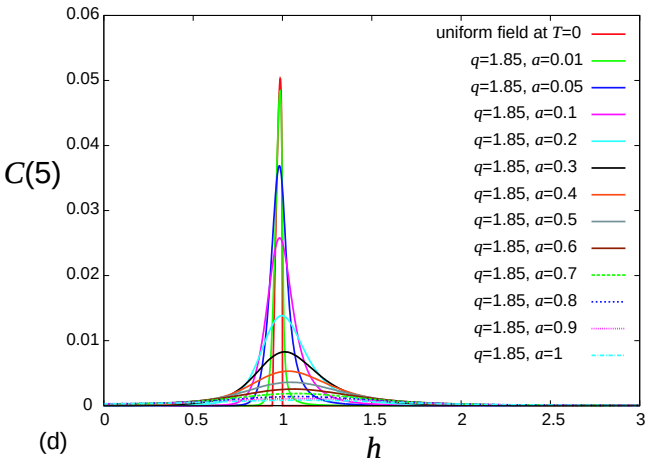

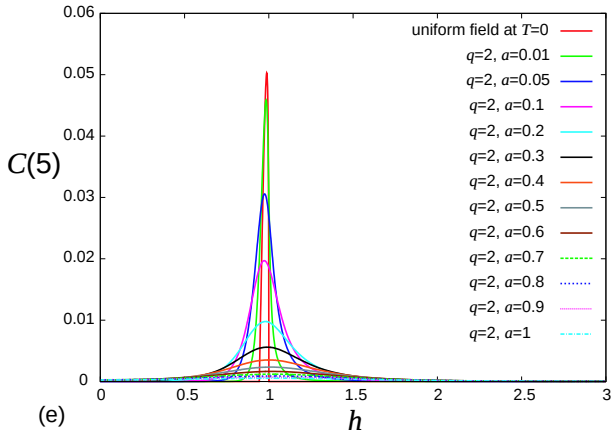

Figure 3.12: (a) The fifth neighbor concurrence for $q = 1$ (Gauss); (b) The fifth neighbor concurrence for $q = 1.35$; (c) The fifth neighbor concurrence for $q = 5/3$; (d) The fifth neighbor concurrence for $q = 1.85$; (e) The fifth neighbor concurrence for $q = 2$ (Lorentz). All the data are plotted as functions of the uniform field for $N = 500$.

3.3.4 The entanglement of the XY model at finite temperature

We finally study the case at finite temperatures and see the difference between the effects of the random magnetic field and the thermal fluctuation on the concurrence. We immediately have Fig. 3.13 for the concurrence at finite T by using the results in §3.2.2, Eqs. (3.3.1), (3.3.9) and (3.3.10).

We can hardly see the difference between the random magnetic field and the thermal fluctuation on the nearest-neighbor concurrence, as shown in Fig. 3.13(a); in the region $h < 1$, the concurrence is decreased by the thermal fluctuation, while in the region $h > 1$, the entanglement is restored by the thermal fluctuation. The reason why the entanglement is restored may be that in $h > 1$ the temperature allows the entangled energy state to exist in some probability by thermal fluctuation. Thus, the concurrence can have non-zero value. On the other hand, the next-nearest neighbor concurrence and the third-neighbor concurrence behave differently depending on whether the disturbance is magnetic or thermal; The restoration of the entanglement in the region $h < 1$ does not appear in the case of the thermal fluctuation.

The maximum point of the next-nearest-neighbor concurrence and the third-neighbor concurrence first shifts to the left and turns to the right; see Fig. 3.13(b) and (c). The effect of the thermal fluctuation on the maximum point of the concurrence is similar to the random magnetic field in the cases of $q > 5/3$.

In Fig. 3.13(c), the third-neighbor concurrence for $\beta^{-1} = 0.8$ and $\beta^{-1} = 1.0$ vanishes in any magnetic field h. Any entanglements vanish in the high-temperature limit, because all the density matrices are reduced to the identity matrix (see Eq. (1.2.5)) and the state described by the identity operator is separable.

The reduction of the maximum point of the concurrences for the random magnetic field or at finite temperatures as a function of the scale parameter or temperature β^{-1} is plotted in Fig. 3.14. The nearest-neighbor concurrence decreases for the random magnetic field more rapidly than at finite temperatures in the plotted ranges. In the same region, however, the third-neighbor concurrence $C(3)$ in the random magnetic field remains finite, whereas the third-neighbor concurrence at finite temperatures almost vanishes for $\beta^{-1} \geq 0.07$. As the distance between the two spins increases, the concurrence becomes weak against the temperature.

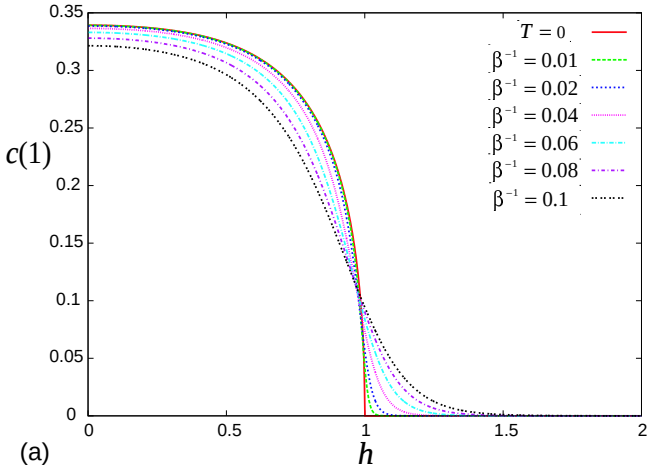
0.35
0.3
0.25
0.2
0.15
0.1
0.05
0
c(1)
0
0.5
1
1.5
2
h
T = 0
β^-1 = 0.01
β^-1 = 0.02
β^-1 = 0.04
β^-1 = 0.06
β^-1 = 0.08
β^-1 = 0.1

(a)

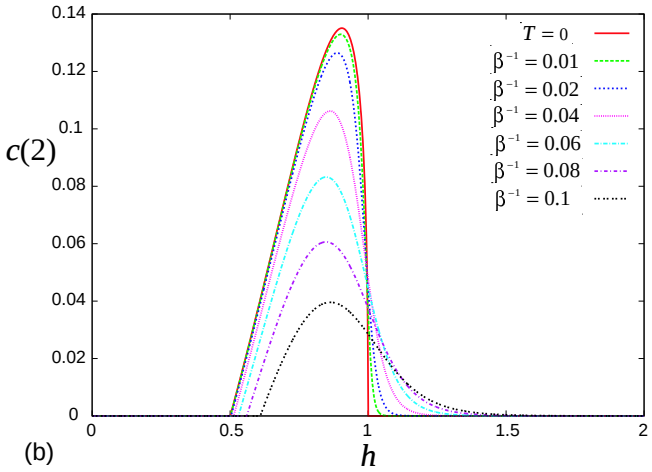
0.14
0.12
0.1
0.08
0.06
0.04
0.02
0
c(2)
0
0.5
1
1.5
2
h
T = 0
β^-1 = 0.01
β^-1 = 0.02
β^-1 = 0.04
β^-1 = 0.06
β^-1 = 0.08
β^-1 = 0.1

(b)

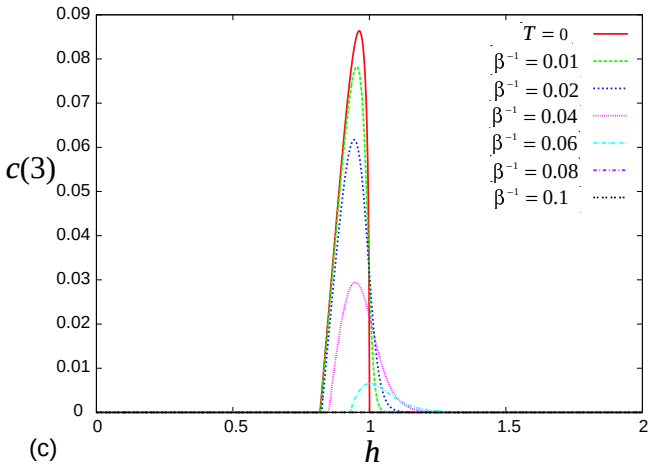

Figure 3.13: (a) The nearest-neighbor concurrence at various temperatures; (b) The next-nearest-neighbor concurrence at various temperatures; (c) The third-neighbor concurrence at various temperature. All the data are plotted as functions of the uniform magnetic field h.

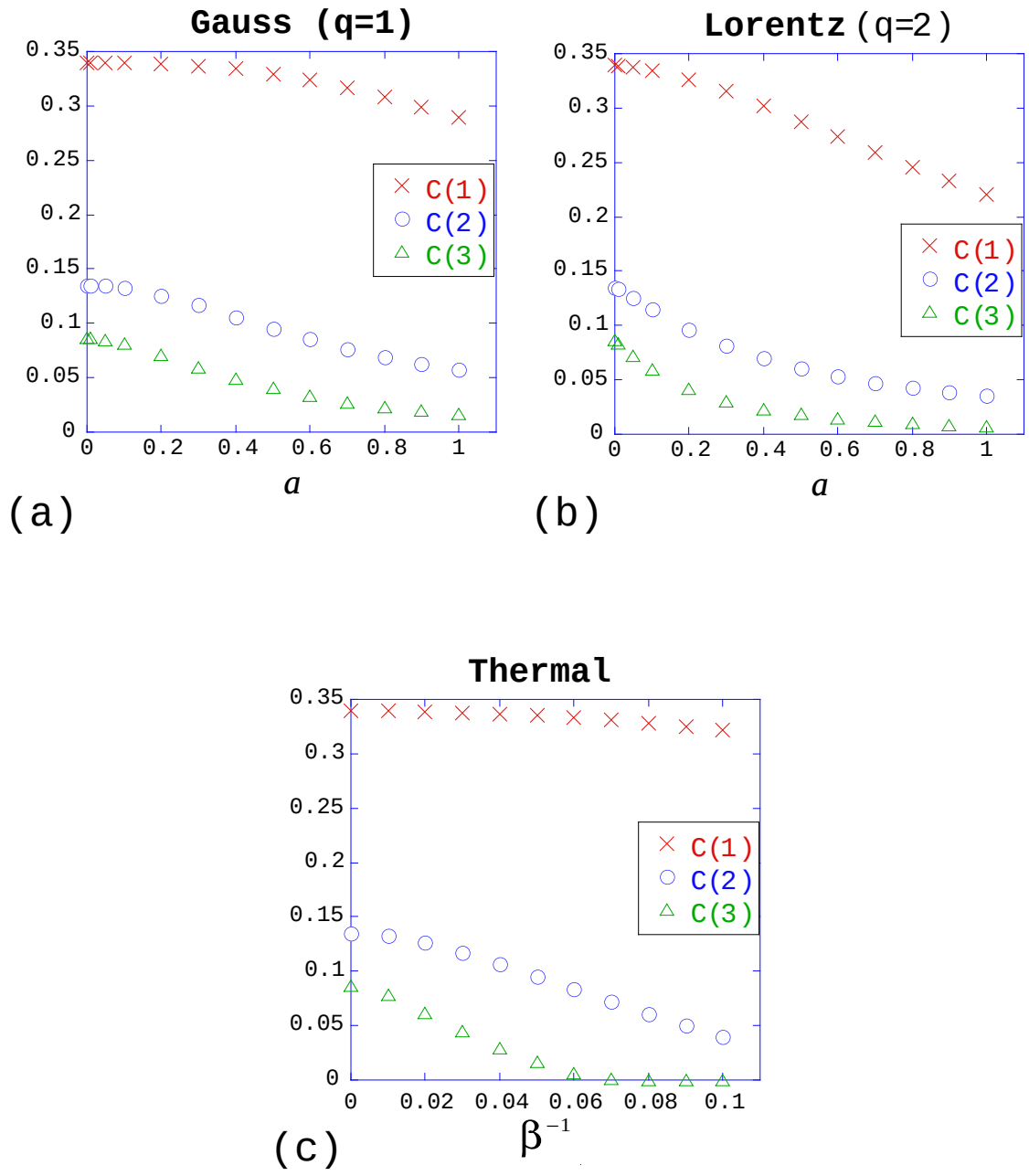

Figure 3.14: (a) The maximum point of the concurrences at finite temperature as a function of the temperature β^{-1}; (b) The maximum point of the concurrences for $q = 1$ as a function of the scale parameter a; (c) The maximum point of the concurrences for $q = 2$ as a function of the scale parameter a.

Chapter 4

Conclusion

To summarize, we have studied the entanglement of the XY spin chain in a random magnetic field. We found that: (i) In general, the entanglement is decreased by randomness; (ii) The entanglement is restored by a random magnetic field in some regions. In particular, we find that the next-nearest-neighbor concurrence in the region $h < 1/2$ is restored by the random magnetic field as well as in the region $h > 1$. The restoration of the concurrence in the region $h < 1/2$ does not occur for the thermal fluctuation. A notable difference between the random magnetic field and the temperature appears in this point. (iii) The qualitative behavior of the concurrence depends on whether the variance of the distribution function is finite or not. In particular, the maximum point of the concurrence shifts to the right when the variance of the distribution function is finite, whereas it shifts to the left when the variance of the distribution function is infinite.

We need further studies to find why the concurrence is restored by random magnetic field and thermal fluctuation, and why the qualitative behavior of the concurrence depends on whether the variance of the random magnetic field is finite or not.

Acknowledgment

I would like to express my gratitude to Professor Naomichi Hatano for his valuable discussions, suggestion and critical reading of the manuscript. I am grateful to Dr. Manabu Machida for his advice on computer programing, Dr. Akinori Nishino for useful suggestions and advice, and Dr. Yukihiro Ota for useful advice. I also acknowledge helps from Dr. Takashi Imamura, Mr. Keita Sasada and Mr. Yuichi Nakamura.

Appendix A

The Schmidt decomposition

In this appendix, we explain the Schmidt decomposition. Suppose that $|\psi\rangle$ is a pure state of a composite system of A and B. Then there exits an orthonormal set $\{|\phi_A^i\rangle\}$ of the subsystem A and an orthonormal set $\{|\varphi_B^i\rangle\}$ of the subsystem B such that

$$|\psi\rangle = \sum_i \lambda_i |\phi_A^i\rangle |\varphi_B^i\rangle, \tag{A.0.1}$$

where $\{\lambda_i\}$ are non-negative real numbers satisfying $\sum_i \lambda_i^2 = 1$. This is the Schmidt decomposition.

For simplicity, we show the Schmidt decomposition in the case where the systems A and B are of the same dimension. The Schmidt decomposition holds in the general case where the dimension of the subsystem A is different from that of the subsystem B.

Let $\{|j_A\rangle\}$ and $\{|k_B\rangle\}$ be orthonormal bases of the subsystem A and the subsystem B, respectively. Then $|\psi\rangle$ can be expanded as

$$|\psi\rangle = \sum_{j,k} a_{jk} |j_A\rangle |k_B\rangle, \tag{A.0.2}$$

where $\{a_{jk}\}$ are generally complex numbers. Next, we use the singular value decomposition. Let A be a square matrix. Then there exist unitary matrices U and V and a diagonal matrix D with non-negative elements such that

$$A = UDV. \tag{A.0.3}$$

This is the singular value decomposition. By using the singular value decomposition, we can write the coefficient matrix a_{jk} as

$$a_{jk} = \sum_l u_{jl} d_{ll} v_{lk}. \tag{A.0.4}$$

Thus $|\psi\rangle$ is rewritten in the form

$$|\psi\rangle = \sum_{j,k,l} u_{jl} d_{ll} v_{lk} |j_A\rangle |k_B\rangle. \tag{A.0.5}$$

Next, we define $|\phi_A^l\rangle = \sum_j u_{jl}|j_A\rangle$, $|\varphi_B^l\rangle = \sum_k v_{lk}|k_B\rangle$ and $\lambda_l \equiv d_{ll}$. Thus, we have

$$|\Psi\rangle = \sum_l \lambda_l |\phi_A^l\rangle |\varphi_B^l\rangle. \tag{A.0.6}$$

Finally, we confirm that $|\phi_A^l\rangle$ and $|\varphi_B^l\rangle$ form orthonormal sets. Taking the inner product of $|\phi_A^l\rangle$ and $|\phi_A^m\rangle$, we have

$$\langle\phi_A^l|\phi_A^m\rangle = \sum_{j,i} u_{jl}^* u_{im} \langle j_A|i_A\rangle = \sum_j u_{jl}^* u_{jm} = \delta_{lm}, \tag{A.0.7}$$

which proves the orthonomality.

Appendix B

Exact solution of the XY model in a uniform field

In this appendix, we review the exact solution [23–26] of the isotropic XY model in a uniform magnetic field and the calculation of the one-point and two-point correlation functions, which are needed for the calculation of entanglement.

B.1 Diagonalizing Hamiltonian

The Hamiltonian is given by

$$H = -J\sum_{j=1}^{N}(S_j^x S_{j+1}^x + S_j^y S_{j+1}^y) - h\sum_{j=1}^{N} S_j^z, \tag{B.1.1}$$

where $S^\alpha = \frac{1}{2}\sigma^\alpha$ $(\alpha = x, y, z)$ with $\{\sigma^\alpha\}$ being the Pauli matrices,

$$\sigma^x = \begin{pmatrix} 0 & 1 \\ 1 & 0 \end{pmatrix}, \quad \sigma^y = \begin{pmatrix} 0 & -i \\ i & 0 \end{pmatrix}, \quad \sigma^z = \begin{pmatrix} 1 & 0 \\ 0 & -1 \end{pmatrix},$$

N is the number of the spins, J (> 0) is the exchange coupling constant, and h is the uniform magnetic field. Here we impose the periodic boundary conditions

$$S_{N+j}^\alpha = S_j^\alpha \quad (\alpha = x, y, z). \tag{B.1.2}$$

With the ladder operators

$$S_j^\pm = S_j^x \pm iS_j^y, \tag{B.1.3}$$

the Hamiltonian (B.1.1) is expressed in the form

$$H = -\frac{J}{2}\sum_{j=1}^{N}(S_j^+ S_{j+1}^- + S_j^- S_{j+1}^+) - h\sum_{j=1}^{N} S_j^z, \tag{B.1.4}$$

because

$$\begin{aligned} S_j^+ S_{j+1}^- &= (S_j^x + iS_j^y)(S_{j+1}^x - iS_{j+1}^y) \\ &= S_j^x S_{j+1}^x + S_j^y S_{j+1}^y + i(S_j^y S_{j+1}^x - S_j^x S_{j+1}^y), \end{aligned} \tag{B.1.5}$$

$$\begin{aligned} S_j^- S_{j+1}^+ &= (S_j^x - iS_j^y)(S_{j+1}^x + iS_{j+1}^y) \\ &= S_j^x S_{j+1}^x + S_j^y S_{j+1}^y - i(S_j^y S_{j+1}^x - S_j^x S_{j+1}^y), \end{aligned} \tag{B.1.6}$$

and hence

$$S_j^x S_{j+1}^x + S_j^y S_{j+1}^y = \frac{S_j^+ S_{j+1}^- + S_j^- S_{j+1}^+}{2}. \tag{B.1.7}$$

Next, we use the Jordan-Wigner Transformation [27], which maps the spin space into the fermionic space. The Jordan-Wigner transformation is given in the form

$$\begin{aligned} S_j^+ &= \prod_{l=1}^{j-1} \exp(-i\pi a_l^\dagger a_l) a_j^\dagger \\ S_j^- &= \prod_{l=1}^{j-1} \exp(i\pi a_l^\dagger a_l) a_j \\ S_j^z &= S_j^+ S_j^- - \frac{1}{2} = a_j^\dagger a_j - \frac{1}{2}\ , \end{aligned} \tag{B.1.8}$$

where $a_j^\dagger$ and a_j are the creation and annihilation operators of a fermion at site j. We can confirm that $a_j^\dagger$ and a_j satisfy the anti-commutation relations $\{a_i, a_j\} = 0$ and $\{a_i^\dagger, a_j\} = \delta_{ij}$ as follows. The inverse transformation of Eq. (B.1.8) is given by

$$a_j^\dagger = (-2)^{j-1} \prod_{i=1}^{j-1} S_i^z S_j^+, \tag{B.1.9}$$

$$a_j = (-2)^{j-1} \prod_{i=1}^{j-1} S_i^z S_j^-. \tag{B.1.10}$$

Using the relations $(S^z)^2 = 1/4$ and $\{S_i^+, S_i^z\} = 0$, we obtain

$$\begin{aligned} a_i a_j^\dagger &= (-2)^{i+j-2} S_i^- \prod_{l=1}^{i-1} S_l^z \prod_{l=1}^{j-1} S_l^z S_j^+ \\ &= (-2)^{i+j-2} \frac{1}{4^{i-1}} S_i^- \prod_{l=i}^{j-1} S_l^z S_j^+ \\ &= (-2)^{i+j-2} \frac{1}{4^{i-1}} S_i^- S_j^+ \prod_{l=i}^{j-1} S_l^z, \end{aligned} \tag{B.1.11}$$

where we assume $i < j$. Similarly, we have for $i < j$

$$\begin{aligned} a_j^\dagger a_i &= (-2)^{i+j-2} S_j^+ \prod_{l=1}^{j-1} S_l^z \prod_{l=1}^{i-1} S_l^z S_i^- \\ &= (-2)^{i+j-2} \frac{1}{4^{i-1}} S_j^+ \prod_{l=i}^{j-1} S_l^z S_i^- \\ &= -(-2)^{i+j-2} \frac{1}{4^{i-1}} S_j^+ S_i^- \prod_{l=i}^{j-1} S_l^z \\ &= -(-2)^{i+j-2} \frac{1}{4^{i-1}} S_i^- S_j^+ \prod_{l=i}^{j-1} S_l^z. \end{aligned} \tag{B.1.12}$$

We thus arrive at the relation $\{a_i^\dagger, a_j\} = 0$ for $i < j$. Taking the Hermite conjugate of the both sides leads us to $\{a_i^\dagger, a_j\} = 0$ for $i > j$. We can similarly show the relation $\{a_i, a_j\} = \{a_i^\dagger, a_j^\dagger\} = 0$.

We now transform the terms $S_j^+ S_{j+1}^-$ and $S_j^- S_{j+1}^+$ with Eq. (B.1.8). Because of the boundary conditions (B.1.2), however, there is a difference between the cases $j \neq N$ and $j = N$. For $j \neq N$, we have

$$S_j^+ S_{j+1}^- = a_j^\dagger \exp(i\pi a_j^\dagger a_j) a_{j+1} = a_j^\dagger a_{j+1}, \tag{B.1.13}$$

$$S_j^- S_{j+1}^+ = a_j \exp(-i\pi a_j^+ a_j) a_{j+1}^\dagger = a_{j+1}^\dagger a_j, \tag{B.1.14}$$

while for $j = N$, we have from Eq. (B.1.2),

$$\begin{aligned} S_N^+ S_1^- &= \prod_{i=1}^{N-1} \exp(-i\pi a_i^\dagger a_i) a^\dagger a_1 \\ &= (1-2n_1)(1-2n_2)\cdots(1-2n_{N-1}) a_N^\dagger a_1 \\ &= (1-2n_1)(1-2n_2)\cdots(1-2n_{N-1})(1-2n_N)^2 a_N^\dagger a_1 \\ &= -(-1)^{N_F} a_N^\dagger a_1, \end{aligned} \tag{B.1.15}$$

and similarly,

$$S_N^- S_1^\dagger = (-1)^{N_F} a_N a_1^\dagger, \tag{B.1.16}$$

where N_F is the number of the fermions,

$$N_F = \sum_{j=1}^{N} n_j, \tag{B.1.17}$$

with n_j being the number operator, $n_j = a_j^\dagger a_j$. In other words, the boundary conditions (B.1.2) is reduced to the signs in Eqs. (B.1.15) and (B.1.16). Thus the Hamiltonian (B.1.4) is transformed to the fermion Hamiltonian

$$H = -\frac{J}{2} \sum_{j=1}^{N} (a_j^\dagger a_{j+1} + a_{j+1}^\dagger a_j) - h \sum_{j=1}^{N} \left(a_j^\dagger a_j - \frac{1}{2} \right), \tag{B.1.18}$$

with

$$\begin{aligned} a_{N+1} = -a_1,\ a_{N+1}^\dagger = -a_1^\dagger \quad &\text{for even } N_F, \\ a_{N+1} = a_1,\ a_{N+1}^\dagger = a_1^\dagger \quad &\text{for odd } N_F. \end{aligned} \tag{B.1.19}$$

Thanks to its translational invariance, we can diagonalize the Hamiltonian (B.1.18) with the Fourier transform

$$\begin{aligned} a_j &= \frac{1}{\sqrt{N}} \sum_k e^{ikj} c_k, \\ a_j^\dagger &= \frac{1}{\sqrt{N}} \sum_k e^{-ikj} c_k^\dagger, \end{aligned} \tag{B.1.20}$$

where we assume that N is even for simplicity. The creation and annihilation operators $c_k^\dagger$ and c_k satisfy the anti-commutation relations

$$\{c_k, c_{k'}\} = 0, \quad \{c_k^\dagger, c_k\} = \delta_{kk'}. \tag{B.1.21}$$

Owing to the boundary conditions (B.1.19), the wave number k can take the values

$$\begin{aligned} k = \pm\frac{\pi}{N},\ \pm\frac{3\pi}{N},\ \cdots,\ \pm\frac{N-1}{N}\pi \quad &\text{for odd } N_F, \\ k = 0,\ \pm\frac{2\pi}{N},\ \pm\frac{4\pi}{N},\ \cdots, \pm\frac{N-2}{N}\pi,\ \pi \quad &\text{for even } N_F. \end{aligned} \tag{B.1.22}$$

Noting the fact that

$$\sum_{j=1}^{N} e^{i(k-k')j} = N\delta_{kk'}, \tag{B.1.23}$$

we can easily confirm the relations (B.1.21).

The hopping term of the Hamiltonian (B.1.18) is now diagonalized in the form

$$\begin{aligned} \sum_{j=1}^{N} (a_j^\dagger a_{j+1} + a_{j+1}^\dagger a_j) &= \frac{1}{N} \sum_{j=1}^{N} \sum_{k,k'} \{c_k^\dagger c_{k'} e^{ik'} e^{-i(k-k')j} + c_k^\dagger c_{k'} e^{-ik} e^{-i(k-k')j}\} \\ &= \sum_{k,k'} (c_k^\dagger c_{k'} e^{-ik'} \delta_{k,k'} + c_{k'}^\dagger c_k e^{ik} \delta_{k,k'}) \\ &= \sum_k 2\cos k\, c_k^\dagger c_k. \end{aligned} \tag{B.1.24}$$

Similarly, we have

$$\begin{aligned} \sum_{j=1}^{N} a_j^\dagger a_j &= \frac{1}{N} \sum_{j=1}^{N} \sum_{k,k'} c_k^\dagger c_{k'} e^{-i(k-k')j} \\ &= \sum_{k,k'} c_k^\dagger c_{k'} \delta_{k,k'} \\ &= \sum_k c_k^\dagger c_k. \end{aligned} \tag{B.1.25}$$

Therefore, the Hamiltonian (B.1.18) is diagonalized as

$$\begin{aligned} H &= -\frac{J}{2}\sum_k 2\cos k\, c_k^\dagger c_k - h\sum_k c^\dagger c_k + \frac{Nh}{2} \\ &= -\sum_k (J\cos k + h) c_k^\dagger c_k + \frac{Nh}{2}. \end{aligned} \tag{B.1.26}$$

B.2 One-point and two-point correlation functions

Now that the Hamiltonian has been diagonalized, we are in the position of calculating the one-point and two-point correlation functions. In the case of the isotropic XYspin chain, we need only the functions $\langle\sigma_i^x\sigma_j^x\rangle = \langle\sigma_i^y\sigma_j^y\rangle$, $\langle\sigma_i^z\sigma_j^z\rangle$ and $\langle\sigma_i^z\rangle$ in order to construct the density matrix.

Equations (B.1.8) and (B.1.3) give the expectation value $\langle\sigma_j^x\sigma_{j+1}^x\rangle_T$ in the form

$$\langle\sigma_j^x\sigma_{j+1}^x\rangle_T = \left\langle (a_i^\dagger + a_i)\exp\left(-i\pi\sum_{l=i}^{j-1}\right)(a_j^\dagger + a_j)\right\rangle_T, \tag{B.2.1}$$

where $\langle\cdots\rangle_T$ denotes the thermal average

$$\langle\cdots\rangle_T = \frac{\mathrm{Tr}(\cdots e^{-\beta H})}{\mathrm{Tr}e^{-\beta H}}. \tag{B.2.2}$$

Noting that $\exp(-i\pi a_i^\dagger a_i) = (a_i^\dagger + a_i)(a_i^\dagger - a_i) = A_iB_i$ and ${A_i}^2 = 1$, we have

$$\langle\sigma_i^x\sigma_j^x\rangle_T = \langle A_iA_iB_iA_{i+1}B_{i+1}A_{i+2}\cdots A_{j-1}B_{j-1}A_j\rangle_T \tag{B.2.3}$$

$$= \langle B_iA_{i+1}B_{i+1}A_{i+2}\cdots A_{j-1}B_{j-1}A_j\rangle_T \tag{B.2.4}$$

where we define A_j and B_j as

$$A_j \equiv a_j^\dagger + a_j, \quad B_j \equiv a_j^\dagger - a_j. \tag{B.2.5}$$

Applying the above procedure, we also have

$$\langle\sigma_i^y\sigma_j^y\rangle_T = \langle B_{i+1}A_iB_{i+2}A_{i+1}\cdots B_jA_{j-1}\rangle_T, \tag{B.2.6}$$

$$\begin{aligned} \langle\sigma_i^z\sigma_j^z\rangle_T &= \langle(2a_i^\dagger a_i - 1)(2a_j^\dagger a_j - 1)\rangle_T \\ &= \langle B_iA_iB_jA_j\rangle_T, \end{aligned} \tag{B.2.7}$$

and

$$\begin{aligned} \langle\sigma_i^z\rangle_T &= \langle(2a_i^\dagger a_i - 1)\rangle_T \\ &= \langle B_iA_i\rangle_T. \end{aligned} \tag{B.2.8}$$

Next, we calculate the correlations (B.2.4), (B.2.6), (B.2.7) and (B.2.8) explicitly. Using Wick's theorem, we can reduce N-point functions into the product of two-point functions $\langle A_l A_m\rangle_T, \langle B_l B_m\rangle_T$ and $\langle B_l A_m\rangle_T$. We first compute the functions $\langle c_k^\dagger c_{k'}\rangle_T$, $\langle c_k c_{k'}\rangle_T$ and $\langle c_k^\dagger c_{k'}^\dagger\rangle_T$ and obtain $\langle A_l A_m\rangle_T$, $\langle B_l B_m\rangle_T$ and $\langle B_l A_m\rangle_T$.

Since the Hamiltonian has been diagonalized as in Eq. (B.1.26), we immediately have

$$\begin{aligned}
&\langle c_k^\dagger c_{k'}^\dagger\rangle_T = \langle c_k c_{k'}\rangle_T = 0 \quad \text{for all } k, k', \\
&\langle c_k^\dagger c_{k'}\rangle_T = \frac{1}{1+\exp(\beta\epsilon(k))}\delta_{kk'},
\end{aligned} \tag{B.2.9}$$

where $\epsilon(k) = -J\cos k - h$ and $\beta = (k_B T)^{-1}$. Noting Eq. (B.1.20), we have

$$\begin{aligned}
\langle A_l A_m\rangle_T &= \langle (a_l^\dagger + a_l)(a_m^\dagger + a_m)\rangle_T \\
&= \frac{1}{N}\langle \sum_{k,k'} (e^{-ikl}c_k^\dagger + e^{ikl}c_k)(e^{-ik'm}c_{k'}^\dagger + e^{ik'm}c_{k'})\rangle_T \\
&= \frac{1}{N}\sum_{k,k'}\left(e^{-ikl+ik'm}\langle c_k^\dagger c_{k'}\rangle_T + e^{ikl-ik'm}\langle c_k c_{k'}^\dagger\rangle_T\right) \\
&= \frac{1}{N}\sum_{k}\left[\frac{e^{-ik(l-m)}}{1+\exp(\beta\epsilon(k))} + e^{ik(l-m)}\left(1 - \frac{1}{1+\exp(\beta\epsilon(k))}\right)\right] \\
&= \frac{1}{N}\sum_{k}\left[\frac{2i\sin k(l-m)}{1+\exp(\beta\epsilon(k))} + N\delta_{lm}\right] \\
&= \delta_{lm},
\end{aligned} \tag{B.2.10}$$

where we use the fact that $\epsilon(k)$ is an even function. Similarly, we have

$$\langle B_l B_m\rangle_T = \delta_{lm}, \tag{B.2.11}$$

$$
\begin{aligned}
\langle B_l A_m \rangle_T &= \langle (a_l^\dagger - a_l)(a_m^\dagger + a_m) \rangle_T \\
&= \frac{1}{N} \langle \sum_{k,k'} (e^{-ikl} c_k^\dagger - e^{ikl} c_k)(e^{-ik'm} c_{k'}^\dagger + e^{ik'm} c_{k'}) \rangle_T \\
&= \frac{1}{N} \sum_{k,k'} \left(e^{-ikl+ik'm} \langle c_k^\dagger c_{k'} \rangle_T - e^{ikl-ik'm} \langle c_k c_{k'}^\dagger \rangle_T \right) \\
&= \frac{1}{N} \sum_k \left[\frac{e^{-ik(l-m)}}{1+\exp(\beta\epsilon(k))} - e^{ik(l-m)} \left(1 - \frac{1}{1+\exp(\beta\epsilon(k))} \right) \right] \\
&= \frac{1}{N} \sum_k \left\{ \frac{2\mathrm{cos}k(l-m)}{1+\exp(\beta\epsilon(k))} - (\mathrm{cos}k(l-m) + i\mathrm{sin}k(l-m)) \right\} \\
&= -\frac{1}{N} \sum_k \mathrm{cos}k(l-m) \frac{1-e^{\beta\epsilon(k)}}{1+e^{\beta\epsilon(k)}} \\
&= -\frac{1}{N} \sum_k \mathrm{cos}k(l-m) \mathrm{tanh}\beta\frac{\epsilon(k)}{2} \\
&= -\frac{1}{2\pi} \frac{2\pi}{N} \sum_k \mathrm{cos}k(l-m) \mathrm{tanh}\beta\frac{\epsilon(k)}{2}.
\end{aligned} \tag{B.2.12}
$$

In the thermodynamic limit $N \to \infty$, the summation over k is replaced by the integral as in

$$
\begin{aligned}
G_{l,m} \equiv \langle B_l A_m \rangle_T &= -\frac{1}{2\pi} \int_{-\pi}^{\pi} \mathrm{d}\phi \, \mathrm{cos}\phi(l-m) \, \mathrm{tanh}\frac{\beta\epsilon(\phi)}{2} \\
&= -\frac{1}{\pi} \int_0^{\pi} \mathrm{d}\phi \, \mathrm{cos}\phi(l-m) \, \mathrm{tanh}\frac{\beta\epsilon(\phi)}{2}.
\end{aligned} \tag{B.2.13}
$$

The function $G_{l,m}$ is divided into two parts:

$$
G_{l,m} = -\frac{1}{\pi} \int_0^{\pi} \mathrm{d}\phi \, \mathrm{cos}(l-m)\phi + \frac{2}{\pi} \int_0^{\pi} \frac{\mathrm{d}\phi}{1+e^{\beta\epsilon(\phi)}}. \tag{B.2.14}
$$

For $l = m$, we have

$$
\begin{aligned}
G_{l,l} &= -\frac{1}{\pi} \int_0^{\pi} \mathrm{d}\phi + \frac{2}{\pi} \int_0^{\pi} \frac{\mathrm{d}\phi}{1+\exp\left[\beta(J\mathrm{cos}\phi + h)\right]} \\
&= -1 + \frac{2}{\pi} \int_0^{\pi} \frac{\mathrm{d}\phi}{1+\exp\left[\beta(J\mathrm{cos}\phi + h)\right]},
\end{aligned} \tag{B.2.15}
$$

while for $l \neq m$, we have

$$
\begin{aligned}
G_{l,m} &= -\frac{1}{\pi} \int_0^{\pi} \mathrm{d}\phi \, \mathrm{cos}(l-m)\phi + \frac{2}{\pi} \int_0^{\pi} \mathrm{d}\phi \frac{\mathrm{cos}(l-m)\phi}{1+\exp\left[-\beta(J\cos\phi + h)\right]} \\
&= \frac{2}{\pi} \int_0^{\pi} \mathrm{d}\phi \frac{\mathrm{cos}(l-m)\phi}{1+\exp\left[-\beta(J\cos\phi + h)\right]}.
\end{aligned} \tag{B.2.16}
$$

Note that the boundary conditions (B.1.22) is irrelevant in the thermodynamic limit.

Now we are ready to calculate the functions $\langle\sigma_i^x\sigma_j^x\rangle$, $\langle\sigma_i^y\sigma_j^y\rangle$, $\langle\sigma_i^z\sigma_j^z\rangle$ and $\langle\sigma_i^z\rangle$. Using Eqs. (B.2.10), (B.2.11), (B.2.16) and Wick's theorem, we can calculate them as follows:

$$\begin{aligned}\langle\sigma_i^x\sigma_j^x\rangle &= \sum_{\tau\in S}\operatorname{sgn}\tau\, G_{i,\tau(i+1)}G_{i+1,\tau(i+2)}\cdots G_{j-1,\tau(j)} \\ &= \begin{vmatrix} G_{-1} & G_{-2} & \cdots & G_{-r} \\ G_0 & G_{-1} & \cdots & G_{-r+1} \\ \vdots & \vdots & \ddots & \vdots \\ G_{r-2} & G_{r-3} & \cdots & G_{-1} \end{vmatrix},\end{aligned} \tag{B.2.17}$$

$$\begin{aligned}\langle\sigma_i^y\sigma_j^y\rangle &= \sum_{\tau\in S}\operatorname{sgn}\tau\, G_{i+1,\tau(i)}G_{i+2,\tau(i+1)}\cdots G_{j,\tau(j-1)} \\ &= \begin{vmatrix} G_1 & G_2 & \cdots & G_r \\ G_0 & G_1 & \cdots & G_{r-3} \\ \vdots & \vdots & \ddots & \vdots \\ G_{-r+2} & G_{-r+3} & \cdots & G_{-1} \end{vmatrix},\end{aligned} \tag{B.2.18}$$

$$\begin{aligned}\langle\sigma_i^z\sigma_j^z\rangle &= \langle B_iA_iB_jA_j\rangle \\ &= \langle B_iA_i\rangle\langle B_jA_j\rangle - \langle B_iA_j\rangle\langle B_jA_i\rangle \\ &= G_0G_0 - G_rG_{-r} \\ &= \begin{vmatrix} G_0 & G_r \\ G_{-r} & G_0 \end{vmatrix},\end{aligned} \tag{B.2.19}$$

$$\begin{aligned}\langle\sigma_i^z\rangle &= \langle 2a_i^\dagger a_i - 1\rangle \\ &= \langle B_iA_i\rangle \\ &= G_0,\end{aligned} \tag{B.2.20}$$

where $\sum_{\tau\in S}$ denotes the summation over all permutations τ and we use the fact that the functions $G_{l,m}$ only depend on the distance $r = l - m$ between the spins. We thus write $G_{l,m}$ as G_{l-m}.

Finally, we investigate the property at zero temperature $T = 0$, or $\beta = \infty$. For $l = m$, the second term of the right-hand side of Eq. (B.2.15) behaves differently, depending on J and h. For $h > J$, we have $J\cos\phi + h > 0$ for all ϕ and thus obtain

$$\lim_{\beta\to\infty}\int_0^\pi \frac{\mathrm{d}\phi}{1+\exp(-\beta\left[J\cos\phi + h\right])} = \int_0^\pi \mathrm{d}\phi = \pi. \tag{B.2.21}$$

For $h < J$, we have

$$\begin{cases} J\cos\phi + h < 0 & \text{for } \arccos(-\frac{h}{J}) < \phi, \\ J\cos\phi + h > 0 & \text{for } 0 < \phi < \arccos(-\frac{h}{J}), \end{cases} \tag{B.2.22}$$

and thus we obtain

$$\lim_{\beta\to\infty} \int_0^\pi \frac{\mathrm{d}\phi}{1+\exp(-\beta\left[J\cos\phi + h\right)]} = \int_0^{\arccos(-\frac{h}{J})} \mathrm{d}\phi = \arccos(-\frac{h}{J}). \tag{B.2.23}$$

Therefore, $G_{l,l}$ behaves as

$$G_{l,l} = \begin{cases} 1 & \text{for } h > J, \\ -1 + \frac{2}{\pi}\arccos(-\frac{h}{J}) & \text{for } h < J. \end{cases} \tag{B.2.24}$$

For $l \neq m$, the right-hand side of Eq. (B.2.16) also behaves differently, depending on J and h. For $h > J$, we again have $J\cos\phi + h > 0$ for all ϕ and thus obtain

$$\lim_{\beta\to\infty} \frac{2}{\pi} \int_0^\pi \mathrm{d}\phi \frac{\cos(l-m)\phi}{1+\exp\left[-\beta(J\cos\phi + h)\right]} = \int_0^\pi \cos(l-m)\phi \mathrm{d}\phi = 0 \tag{B.2.25}$$

For $h < J$, we have Eq. (B.2.22) again and obtain

$$\begin{aligned} \lim_{\beta\to\infty} \frac{2}{\pi} \int_0^\pi \mathrm{d}\phi \frac{\cos(l-m)\phi}{1+\exp\left[-\beta(J\cos\phi + h)\right]} &= \int_0^{\arccos(-\frac{h}{J})} \cos(l-m)\phi \mathrm{d}\phi \\ &= \frac{1}{l-m} \sin\left[(l-m)\arccos\left(-\frac{h}{J}\right)\right]. \end{aligned}$$

Therefore, the function $G_{l,m}$ takes the values

$$G_{l,m} = \begin{cases} 0 & \text{for } h > J, \\ \frac{2}{\pi}\frac{1}{l-m}\sin[(l-m)\arccos(-\frac{h}{J})] & \text{for } h < J. \end{cases} \tag{B.2.26}$$

Appendix C

Numerical solution of the XY model in a random magnetic field at temperature $T = 0$

In this appendix, we consider the XY model in a random magnetic field. We find formulas to calculate the one-point and two-point correlation functions numerically.

C.1 Diagonalizing the Hamiltonian

The Hamiltonian that we consider is given in the form

$$H = -J\sum_{j=1}^{N}(S_j^x S_{j+1}^x + S_j^y S_{j+1}^y) - \sum_{j=1}^{N}(h+h_j)S_j^z, \tag{C.1.1}$$

where h is a uniform field and each h_j is a random magnetic field obeying the probability distribution (3.1.3). As in the case of the previous appendix, we use the Jordan-Wigner transformation (B.1.8) and transform the Hamiltonian (C.1.1) into

$$H = -\frac{J}{2}\sum_{j=1}^{N}(a_j^\dagger a_{j+1} + a_{j+1}^\dagger a_j) - \sum_{j=1}^{N}(h+h_j)\left(a_j^\dagger a_j - \frac{1}{2}\right) \tag{C.1.2}$$

with

$$\begin{aligned} &a_{N+1} = -a_1, \quad a_{N+1}^\dagger = -a_1^\dagger \qquad \text{for even } N_F, \\ &a_{N+1} = a_1, \quad\ \ a_{N+1}^\dagger = a_1^\dagger \qquad\ \ \text{for odd } N_F, \end{aligned} \tag{C.1.3}$$

where N_F is the number of the fermions. The Hamiltonian without the constant term can be written in the form

$$H' = \sum_{j,k} a_j^\dagger A_{j,k} a_k \tag{C.1.4}$$

$$= \boldsymbol{a}^\dagger A \boldsymbol{a}, \tag{C.1.5}$$

with

$$A = \begin{pmatrix} -h-h_1 & -\frac{J}{2} & 0 & \cdots & 0 & \pm\frac{J}{2} \\ -\frac{J}{2} & -h-h_2 & -\frac{J}{2} & 0 & \vdots & 0 \\ 0 & -\frac{J}{2} & \ddots & \ddots & 0 & \vdots \\ \vdots & 0 & \ddots & \ddots & -\frac{J}{2} & 0 \\ 0 & \vdots & \ddots & -\frac{J}{2} & -h-h_{N-1} & -\frac{J}{2} \\ \pm\frac{J}{2} & 0 & \cdots & 0 & -\frac{J}{2} & -h-h_N \end{pmatrix}, \tag{C.1.6}$$

where the signs of the $(1, N)$ and $(N, 1)$ matrix elements depend on the boundary conditions (C.1.3); the sign is negative for even N_F and is positive for odd N_F. The vectors $\boldsymbol{a}$ and $\boldsymbol{a}^\dagger$ denote

$$\boldsymbol{a} = \begin{pmatrix} a_1 \\ a_2 \\ \vdots \\ a_{N-1} \\ a_N \end{pmatrix}, \quad \boldsymbol{a}^\dagger = \begin{pmatrix} a_1^\dagger & a_2^\dagger & \cdots & a_{N-1}^\dagger & a_N^\dagger \end{pmatrix}. \tag{C.1.7}$$

As the matrix (C.1.6) is Hermitian, there exists a unitary matrix V such that $V^\dagger A V = \Lambda$ is a diagonal matrix. We thus have

$$H' = \boldsymbol{a}^\dagger A \boldsymbol{a} = \boldsymbol{c}^\dagger \Lambda \boldsymbol{c} \tag{C.1.8}$$

with

$$\begin{aligned} c_i^\dagger &= \sum_j a_j^\dagger V_{ji}, \\ c_i &= \sum_j V_{ij}^\dagger a_j. \end{aligned} \tag{C.1.9}$$

We here also write the inverse relations of Eq. (C.1.9):

$$\begin{aligned} a_j^\dagger &= \sum_m c_m^\dagger V_{mj}^\dagger, \\ a_j &= \sum_m V_{jm} c_m. \end{aligned} \tag{C.1.10}$$

It is easy to confirm that $c_i^\dagger$ and c_i satisfy the anti-commutation relations $\{c_i^\dagger, c_j\} = \delta_{ij}$ and $\{c_i, c_j\} = 0$. We here show the former relation $\{c_i^\dagger, c_j\} = \delta_{ij}$ for example. From Eq. (C.1.9), we have

$$\begin{aligned} \{c_i^\dagger, c_j\} &= \sum_{l,m} a_l^\dagger V_{li} V_{jm}^\dagger a_m + \sum_{l,m} V_{jm}^\dagger a_m a_l^\dagger V_{li} \\ &= \sum_{l,m} (\delta_{lm} - a_m a_l^\dagger) V_{li} V_{jm}^\dagger + \sum_{l,m} V_{jm}^\dagger a_m a_l^\dagger V_{li} = \delta_{ij}. \end{aligned} \tag{C.1.11}$$

The latter case $\{c_i, c_j\} = 0$ can be shown in a similar way.

C.2 One-point and two-point correlation functions at $T = 0$

Once we diagonalize the matrix (C.1.6), we can construct the many-body ground state of the Hamiltonian (C.1.2). Let $\epsilon_1, \epsilon_2, \cdots \epsilon_{N_G}, \epsilon_{N_G}, \cdots \epsilon_{N-1}, \epsilon_N$ denote the eigenvalues of the matrix (C.1.6) in the ascending order. If $\epsilon_{N_G} < 0$ and $\epsilon_{N_G+1} > 0$, the ground state of the Hamiltonian (C.1.2) is given by

$$|\mathrm{Gs}\rangle = c^\dagger_{N_G} c^\dagger_{N_G-1} \cdots c^\dagger_2 c^\dagger_1 |0\rangle. \tag{C.2.1}$$

We are now in the position of calculating the one-point and two-point correlation functions. We apply the same procedure as in Appendix B to have $\langle \mathrm{Gs}|A_m A_l|\mathrm{Gs}\rangle$, $\langle \mathrm{Gs}|B_m B_l|\mathrm{Gs}\rangle$ and $\langle \mathrm{Gs}|B_m A_l|\mathrm{Gs}\rangle$.

From Eq. (C.1.10) and (C.2.1), we calculate them as follows;

$$\begin{aligned}
\langle \mathrm{Gs}|A_m A_l|\mathrm{Gs}\rangle &= \langle \mathrm{Gs}|(a^\dagger_m + a_m)(a^\dagger_l + a_l)|\mathrm{Gs}\rangle \\
&= \langle \mathrm{Gs}|\sum_i (c^\dagger_i V^\dagger_{im} + V_{mi} c_i) \sum_j (c^\dagger_j V^\dagger_{jl} + V_{lj} c_j)|\mathrm{Gs}\rangle \\
&= \langle \mathrm{Gs}|(\sum_{i,j} c^\dagger_i c_j V^\dagger_{im} V_{lj} + \sum_{i,j} c_i c^\dagger_j V_{mi} V^\dagger_{jl}|\mathrm{Gs}\rangle \\
&= \sum_i^{N_G} V^\dagger_{im} V_{li} + \sum_{i,j} V_{mi} V^\dagger_{jl} \langle \mathrm{Gs}|(\delta_{ij} - c^\dagger_j c_i)|\mathrm{Gs}\rangle \\
&= \delta_{ml},
\end{aligned} \tag{C.2.2}$$

$$\begin{aligned}
\langle \mathrm{Gs}|B_m B_l|\mathrm{Gs}\rangle &= \langle \mathrm{Gs}|(a^\dagger_m - a_m)(a^\dagger_l - a_l)|\mathrm{Gs}\rangle \\
&= \langle \mathrm{Gs}|\sum_i (c^\dagger_i V^\dagger_{im} - V_{mi} c_i) \sum_j (c^\dagger_j V^\dagger_{jl} - V_{lj} c_j)|\mathrm{Gs}\rangle \\
&= -\delta_{ml},
\end{aligned} \tag{C.2.3}$$

and

$$\begin{aligned}
\langle \mathrm{Gs}|B_m A_l|\mathrm{Gs}\rangle &= \langle \mathrm{Gs}|(a^\dagger_m - a_m)(a^\dagger_l + a_l)|\mathrm{Gs}\rangle \\
&= \langle \mathrm{Gs}|\sum_i (c^\dagger_i V^\dagger_{im} - V_{mi} c_i) \sum_j (c^\dagger_j V^\dagger_{jl} + V_{lj} c_j)|\mathrm{Gs}\rangle \\
&= 2\sum_i^{N_G} V_{mi} V_{li} - \delta_{ml}.
\end{aligned} \tag{C.2.4}$$

As in Eq. (B.2.4), we have

$$\begin{aligned}
\langle \mathrm{Gs}|\sigma^x_i \sigma^x_j|\mathrm{Gs}\rangle &= \langle \mathrm{Gs}|\sigma^x_i \sigma^x_{i+1} \sigma^x_{i+1} \cdots \sigma^x_{j-1} \sigma^x_{j-1} \sigma^x_j|\mathrm{Gs}\rangle \\
&= \langle \mathrm{Gs}|B_i A_{i+1} B_{i+1} A_{i+2} \cdots A_{j-1} B_{j-1} A_j|\mathrm{Gs}\rangle.
\end{aligned} \tag{C.2.5}$$

The other correlation functions are also written as in Eqs. (B.2.6), (B.2.7) and (B.2.8), respectively. With the help of Wick's theorem and Eqs. (C.2.2), (C.2.3) and (C.2.4), we arrive at one-point and two-point correlation functions in the form

$$\langle \sigma_i^x \sigma_j^x \rangle = \begin{vmatrix} G_{i,i+1} & G_{i,i+2} & \cdots & G_{i,j} \\ G_{i+1,i+1} & G_{i+1,i+2} & \cdots & G_{i+1,j} \\ \vdots & \vdots & \ddots & \vdots \\ G_{j-1,i+1} & G_{j-1,i+2} & \cdots & G_{j-1,j} \end{vmatrix}, \tag{C.2.6}$$

$$\langle \sigma_i^y \sigma_j^y \rangle = \begin{vmatrix} G_{i+1,i} & G_{i+2,i} & \cdots & G_{j,i} \\ G_{i+1,i+1} & G_{i+2,i+1} & \cdots & G_{j,i+1} \\ \vdots & \vdots & \ddots & \vdots \\ G_{i+1,j-1} & G_{i+2,j-1} & \cdots & G_{j,j-1} \end{vmatrix}, \tag{C.2.7}$$

$$\langle \sigma_i^z \sigma_j^z \rangle = \begin{vmatrix} G_{i,i} & G_{i,j} \\ G_{j,i} & G_{j,j} \end{vmatrix}, \tag{C.2.8}$$

$$\langle \sigma_i^z \rangle = G_{i,i}, \tag{C.2.9}$$

where

$$G_{i,j} = 2 \sum_{l=1}^{N_G} V_{il} V_{jl} - \delta_{ij}. \tag{C.2.10}$$

Bibliography

[1] C. H. Bennet, G. Brassard, C. Crépeau, R. Jozsa, A. Peres, and W. K. Wootters, Phys. Rev. Lett. **70**, 1895 (1993)

[2] M. A. Nielsen and I. L. chuang, *Quantum Computation and Quantum Information* (Cambridge University Press, Cambridge, 2000)

[3] C. H. Bennett, and S. J. Wiesner, Phys. Rev. Lett. **69**, 2881 (1992)

[4] A. Einstein, B. Podolsky, and N. Rosen, Phys. Rev. **47**, 777 (1935)

[5] J. S. Bell, Physics **1**, 195 (1964)

[6] J. F. Clauser, M. A Horne, A. Shimony, and R. A. Holt, Phys. Rev. Lett. **23**, 880 (1969)

[7] A. Osterloh, L. Amico, G. Falcl, and R. Fazio, Nature **416**, 608 (2002)

[8] T. J. Osborne and M. A. Nielsen Phys. Rev. A **66**, 032110 (2002)

[9] H. Yano and H. Nishmori, Prog. Theor. Phys. suppl. **157**, 164 (2005)

[10] H. Yano, *The entanglement of the quantum spin chain in the uniform field* (Master thesis, Tokyo Institute of Technology, 2006)

[11] S. J. Gu, S. S. Deng, Y. Q. Li, and H. Q. L Phys. Rev. Lett. **93**, 086402 (2004)

[12] M. C. Arnesen, S. Bose, and V. Vedral, Phys. Rev. Lett. **87**, 017901 (2001)

[13] D. Boschi, S.Branca, F. D. Marini, L. Hardy, and S. Popescu, Phys. Rev. Lett. **80**, 1121 (1998)

[14] D. Bouwmeester, J. W. Pan, K. Mattle, M. Eibl, H. Weinfurter, and A. Zeilinger, Nature **390**, 575 (1997)

[15] A. Furusawa, J. L. Sørensen, S. L. Braunstein, C. A. Fuchs, H. J. kimble, and E. S. Polzik, Science **282**, 706 (1998)

[16] M. A. Nielsen, E. Knill, and R. Laflamme, Nature **396**, 52 (1998)

[17] C. H. Bennett, H. J. Bernstein, S. Popescu, and B. Schumacher, Phys. Rev. A **53**, 2046 (1996)

[18] C. H. Bennett, G. Brassard, S. Popescu, B. Schumacher, J. Smolin, and W. K. Wootters, Phys. Rev. Lett. **76**, 722 (1996)

[19] C. H. Bennett, D. P. DiVincenzo, J. A. Smolin and W. K. Wootters, Phys. Rev. A **54**, 3824 (1996)

[20] W. K. Wootters, Quan. Inf. Comp. **1**, 27 (2001)

[21] M. Horodecki, Quan. Inf. Comp. **1**, 3 (2001)

[22] W. K. Wootters, Phys. Rev. Lett. **80**, 2245 (1998)

[23] E. Barouch and B. M. McCoy, Phys. Rev. A **2**, 1075 (1970)

[24] T. Oguchi and I. Ono, J. Phys. Soc. Jpn. **26**, 1378 (1969)

[25] B. K. Chakrabarti, A. Dutta, and P. Sen, *Quantum Ising Phases and Transitions in Transverse Ising Models* (Springer-Verlag, Berlin, 1996)

[26] H. Nishimori, *Soutenni rinnkai gennsyouno toukei buturigaku* (Baifuukan, Tokyo, 2005)

[27] P. Jordan and E. Wigner, Z. Phys. **47**, 631 (1928)

[28] H. Nishimori, Phys. Lett. **100A**, 239 (1984)

[29] M. A. Nielsen, e-print quant-ph/0011036